Classroom Photocopying Permission

Chapters from Teaching General Chemistry: A Materials Science Companion. Copyright © 1993 American Chemical Society. All Rights Reserved.
For reproduction of each chapter for classroom use, contact the American Chemical Society or report your copying to the Copyright Clearance Center, Inc., 222 Rosewood Drive, Danvers, MA 01923.

Experiments from Teaching General Chemistry: A Materials Science Companion. Copyright © 1993 American Chemical Society. All Rights Reserved. Multiple copies of the experiments may be made for classroom use only, provided that the following credit line is retained on each copy: "Reproduced with permission from *Teaching General Chemistry: A Materials Science Companion*." You may edit the experiments for your particular school or class and make photocopies of the edited experiments, provided that you use the following credit line: "Adapted with permission from *Teaching General Chemistry: A Materials Science Companion*."

Overhead Masters
Multiple copies of the overhead masters may be made for classroom use only, provided that the extant credit lines are retained on each copy: "© 1993 American Chemical Society. Reproduced with permission from *Teaching General Chemistry: A Materials Science Companion*" or "© 1995 by the Division of Chemical Education, Inc., American Chemical Society. Reproduced with permission from *Solid-State Resources* ."

Laboratory Safety

DISCLAIMER

Safety information is included in each chapter of the Companion as a precaution to the readers. Although the materials, safety information, and procedures contained in this book are believed to be reliable, they should serve only as a starting point for laboratory practices. They do not purport to specify minimal legal standards or to represent the policy of the American Chemical Society. No warranty, guarantee, or representation is made by the American Chemical Society, the authors, or the editors as to the accuracy or specificity of the information contained herein, and the American Chemical Society, the authors, and the editors assume no responsibility in connection therewith. The added safety information is intended to provide basic guidelines for safe practices. Therefore, it cannot be assumed that necessary warnings or additional information and measures may not be required. Users of this book and the procedures contained herein should consult the primary literature and other sources of safe laboratory practices for more exhaustive information. See page xxv in the Text 0 Preface file in the Companion Text folder for more information.

Chapter 9

Applications of Thermodynamics: Phase Changes

Phase changes include interconversions of solids, liquids, and gases, as in, for example, ice melting to liquid water and solid carbon dioxide (dry ice) subliming into the gaseous state. There are many technologically important classes of phase changes, however, that occur exclusively in the solid state.

In this chapter, after a qualitative discussion using Le Chatelier's principle to interpret the effects of temperature and pressure on equilibria involving solids, three types of solid-state phase changes will be presented. The first, involving NiTi "memory metal," is representative of a class of phase changes called martensitic transformations, wherein changes in temperature and pressure (mechanical stress) can cause a reversible shift of atomic positions in the crystal that leads to remarkable changes in mechanical properties. The second, based on the $YBa_2Cu_3O_{7-x}$ superconductor, highlights a phase change characterized by a pairing of electrons that results in striking changes in electromagnetic properties. Finally, temperature-induced changes in ionic conductivity and optical properties arise from a solid-state phase change in Cu_2HgI_4 that involves shifting from an ordered arrangement of cations to a disordered arrangement, a so-called "order-disorder" phase change.

Additional solid-state phase transformations include the conversions between hexagonal close-packed and face-centered cubic (fcc) structures in metals (Chapter 5) and interactions of electrons in magnetic garnets (*see* Experiment 13).

2725-X/93/0277$13.80/1 © 1993 American Chemical Society

Chapter 9

Applications of Thermodynamics: Phase Changes

Phase changes include interconversions of solids, liquids, and gases, as in, for example, ice melting to liquid water and solid carbon dioxide (dry ice) subliming into the gaseous state. There are many technologically important classes of phase changes, however, that occur exclusively in the solid state.

In this chapter, after a qualitative discussion using Le Chatelier's principle to interpret the effects of temperature and pressure on equilibria involving solids, three types of solid-state phase changes will be presented. The first, involving NiTi "memory metal," is representative of a class of phase changes called martensitic transformations, wherein changes in temperature and pressure (mechanical stress) can cause a reversible shift of atomic positions in the crystal that leads to remarkable changes in mechanical properties. The second, based on the $YBa_2Cu_3O_{7-x}$ superconductor, highlights a phase change characterized by a pairing of electrons that results in striking changes in electromagnetic properties. Finally, temperature-induced changes in ionic conductivity and optical properties arise from a solid-state phase change in Cu_2HgI_4 that involves shifting from an ordered arrangement of cations to a disordered arrangement, a so-called "order-disorder" phase change.

Additional solid-state phase transformations include the conversions between hexagonal close-packed and face-centered cubic (fcc) structures in metals (Chapter 5) and interactions of electrons in magnetic garnets (*see* Experiment 13).

Effects of Temperature and Pressure on Equilibria: Illustrations of Le Chatelier's Principle with Solids

Qualitative discussions of chemical equilibrium typically focus on the effects of concentration and temperature on gaseous and solution equilibria and of pressure or volume changes on gaseous equilibria. Solids often are discussed in connection with heterogeneous equilibria such as solubility equilibria, where the point is made, seemingly paradoxically at first, that solids can be ignored so long as they are present!

In fact, in addition to the electronic and ionic-based equilibria described in Chapter 8, solids engage in a variety of pressure- and temperature-dependent equilibria that enrich the qualitative predictions afforded by Le Chatelier's principle. A practical example involving nickel–titanium memory metal appears later in this chapter, but some general illustrations involving phase changes are given first.

The free energy, *G*, of a pure material can be used to predict which phase of the substance is favored at different combinations of pressure and temperature: At a given pressure and temperature, the phase having the lowest free energy will be the most stable phase. Le Chatelier's principle provides a means for predicting pressure and temperature effects: Equilibria of endothermic reactions shift to products with an increase in temperature, and an increase in pressure shifts the equilibrium to favor the denser phase. The free-energy changes corresponding to the predictions reflect entropy and volume considerations that are discussed briefly in Appendix 9.1.

The equilibrium involving liquid water and ice (eq 1) illustrates both temperature and pressure effects. As commonly written,

$$\text{reaction energy} + \underset{\text{less dense}}{H_2O_{(s)}} \rightleftarrows \underset{\text{more dense}}{H_2O_{(l)}} \qquad (1)$$

Le Chatelier's principle predicts that heat added to an ice–water mixture at equilibrium will convert some of the ice to liquid water.

For the same reaction, there is also a volume change, because ice is less dense than water, as illustrated by the flotation of ice in water. The conversion of water to ice can produce mechanical work, as is sometimes spectacularly illustrated by the volume increase accompanying freezing in an "ice bomb" *(1)*. In general, the direction of a chemical equilibrium that yields a volume increase can be used to perform mechanical or pressure–volume "PV" work.[1]

---

[1]The actual magnitude of mechanical energy effects is generally much smaller than thermal energy effects: even when large pressures are involved, they are often coupled to small volume changes so that the product of pressure and volume is a modest energy change.

Le Chatelier's principle predicts that if external pressure is applied to ice, the system will respond by shifting the equilibrium to favor the phase having greater density, which is liquid water. The ability to ice skate is partially attributable to the fact that pressure from the ice skate blade can help reduce friction by pushing the equilibrium toward formation of liquid water, and thus effectively lower the melting point of H_2O. References 2 and 3 present further discussion of the effects of the ice–water equilibrium applicable to skating and Demonstration 9.1.

A material with a similar property is elemental gallium, which melts at about 30 °C. Like H_2O, gallium expands on freezing. In principle, it should be possible to skate on a gallium rink. Of course, skate blades that do not react with the liquid metal would be needed!

Demonstration 9.1. The Effect of Pressure on the Melting Point of Ice

Materials

Iron pipe (1-inch diameter) and a rubber stopper (the length of pipe is not critical but a 1-foot-long piece works well)
Two ring stands and clamps
28-gauge copper wire (1-foot length)
Two 1-kg weights
Two foam blocks with notches cut in them

Procedure

- Prepare a cylinder of ice by placing a stopper in one end of the pipe, adding water until the pipe is full, and placing this container upright in a freezer. The ice may be removed from the pipe by passing warm water over the outside.
- Place the ring stands about 8 inches apart. Clamp the foam blocks and position the cylinder of ice in the grooves of the foam like the crossbar of a goalpost.
- Tie a 1-kg weight to each end of the wire. There should be about 10 inches of wire between the two weights.
- Hang the wire and weights over the piece of ice so that one weight will be on each side of the cylinder. The wire will begin to cut through the ice as the pressure from the mass of the wire and weights melts the ice.
- After 2–3 minutes the wire will have passed through the ice and the weights will fall to the floor. (You may want to place rags on the floor to lessen the noise when the weights fall.) The water above the cut will have refrozen.
- Show that the ice cylinder can be lifted off the support in one piece after the wire passes through and the pressure is removed.

The same principles can be applied to transformations occurring exclusively in the solid state. For all of the examples that follow, external pressure can be used to convert the less dense to the more dense phase. A typical illustration is the conversion of bcc to fcc metals:

$$\underset{\text{less dense}}{\text{bcc}} \rightleftarrows \underset{\text{more dense}}{\text{fcc}} \qquad (2)$$

The bcc packing efficiency is only 68%, and the fcc packing efficiency is 74%, so that an increase in pressure favors the close-packed fcc structure (Chapter 5).

A second example is the pressure-induced conversion of graphite to diamond, a method by which synthetic diamonds are made at high temperature. Pressure can be used to overcome the unfavorable enthalpy and entropy changes associated with this transformation. The Solid-State Model Kit can be used to build both graphite and diamond and to directly compare their packing efficiencies.

$$\text{reaction energy} + \underset{\text{less dense}}{\text{graphite (s)}} \rightleftarrows \underset{\text{more dense}}{\text{diamond (s)}} \qquad (3)$$

[As noted in Chapter 1, there are now ways to produce diamond films, relatively inexpensively, by chemical vapor deposition methods (Chapter 10)].

An example of a phase change with historical significance is the conversion of less dense α-tin ("gray tin"; cubic diamond structure, Chapter 5) to denser β-tin ("white tin"; a tetragonal structure having a unit cell with a square base and rectangular sides), which occurs a little below room temperature.

$$\text{reaction energy} + \underset{\text{less dense}}{\text{α-tin (s)}} \rightleftarrows \underset{\text{more dense}}{\text{β-tin (s)}} \qquad (4)$$

In early European cathedrals, organ pipes made of tin were found to swell and then to disintegrate in cold weather *(4)*. The origin of this so-called "tin disease" is the phase transformation of tin: Low temperatures shift the equilibrium toward α-tin, and the lower density of this phase results in swelling and ultimately disintegration from the relatively large shifts in atomic position that are demanded by the phase transformation.

The phase changes that salts and minerals undergo are also important in understanding geological processes. The transformation of sodium chloride, for example, from the rock salt to the cesium chloride structure, equation 5, can be accomplished at 298 K at high pressure (~10^5 atm) *(5)*:

$$\underset{\text{less dense}}{\text{NaCl (rock salt structure)}} \rightleftarrows \underset{\text{more dense}}{\text{NaCl (cesium chloride structure)}} \qquad (5)$$

An important feature of solid-state phase changes that distinguish them from many other phase changes is that superheating and supercooling are extremely common, being more the rule than the exception. Recall

that solid-to-liquid phase changes like ice to liquid water occur abruptly at a well-defined temperature and pressure for pure samples. However, liquids can be supercooled, freezing substantially below their normal melting point, if a nucleation site for the growth of ice crystals is unavailable.[2] Similarly, liquids can be superheated, boiling above their normal boiling point, if a nucleation site for bubble formation is absent.

In solid-state phase changes, superheating and supercooling are common, because the new phase generally has to nucleate and grow within the phase that is initially present. The shifts in atomic position that are required for this growth are relatively slow, particularly if diffusion is required at temperatures near and below room temperature (*see* Chapter 10). Ultimately, the energy requirement for the growth of the new phase is met by shifting the temperature and/or pressure enough beyond the point of thermodynamic equilibrium through superheating or supercooling that sufficient chemical free energy is available to complete the structural conversion.

Nickel–Titanium Memory Metal

A captivating property of the alloy NiTi is its ability to "remember" a shape into which it has previously been fabricated *(7)*. The processes underlying the shape-memory effect illustrate links between the structure, microstructure, and composition of NiTi (the stoichiometry of the solid can vary by a few percent from 1:1 Ni:Ti) and general thermodynamic principles of phase transformations.

Samples of NiTi readily undergo a martensitic phase transformation, a kind of ballet on the atomic scale: atoms in solids like NiTi can make subtle orchestrated shifts in their positions, which, because little energy is involved, can occur in the vicinity of room temperature and below. In any martensitic phase transformation the high-temperature phase is called austenite, and the low temperature phase is called martensite, regardless of the crystal structures of the phases. This nomenclature was originally derived from the martensitic phase transformation in steel (Chapter 6).

Of the many alloys that exhibit the shape-memory effect, *(8, 9)* the "memory metal" comprising nickel and titanium atoms is one of the most accessible and dramatic. Memory metal is sometimes called nitinol, which is short for **ni**ckel **ti**tanium **N**aval **O**rdnance **L**aboratory and which acknowledges the site of its discovery in 1965 *(10)*. The relatively low cost of the alloy and its ready availability make it ideal for lecture demonstrations and laboratory experiments in general chemistry courses. In addition to illustrating the martensitic phase change, the ability of NiTi to remember its shape under certain experimental conditions makes it an

[2]The related phenomenon of supersaturation can be demonstrated by using sodium acetate solution or sodium thiosulfate solutions. *See* reference 6.

entry point for discussing "smart" materials. "Smart" materials have the capability to sense changes in their environment and respond to the changes in a preprogrammed way. These new high-tech solids are being used in a variety of artistic, medical, and engineering applications.

The Structural Cycle of Shape Memory

As described in Demonstration 9.2, thin, straight wires and rods of NiTi display an astonishing, counterintuitive property: they can be distorted into a variety of shapes while in their low-temperature phase at room temperature, then, upon gentle warming into the high-temperature phase, the samples will return to their original shape. Cooling the sample from its high-temperature phase into its low-temperature phase will not generally cause an observable change in its shape.

Demonstration 9.2. The Shape-Memory Property of Memory Metal

Materials

NiTi wire (3 inches long by 0.03 inches in diameter works well) with transition temperatures between 30 and 50 °C; *see* Supplier Information
Hot water (over 50 °C) in a crystallizing dish or small beaker (or heat gun or hair dryer)
Gloves or tongs (optional)
Tape (optional)
Overhead projector and screen (optional)
9-V battery (optional)
Battery snap with alligator clips attached to the leads (optional)
Sample of memory metal that spells "ICE" (available from the Institute for Chemical Education) (optional)
3–6-V power supply (such as a lantern battery) and leads with alligator clips (optional)

Procedure

- Place a sample of low-temperature phase martensite NiTi wire on the overhead projector to show its linear shape.
- Bend it; for a particularly dramatic demonstration, coil the wire around a finger to form a helical shape.
- Then, holding one end of the coiled wire, immerse it in hot water. (Alternatively, place it in the hot-air stream of a hair dryer. As a third option, while wearing gloves or holding the wire with tongs, place the wire in the hot-air stream of a heat gun.) As the wire is heated, it transforms into the austenite phase and straightens back

into the linear shape it had been "trained" to remember.

Variations

To demonstrate this effect in a large lecture room, place a crystallizing dish containing hot water on an overhead projector so that the straightening of the wire is readily visible. Alternatively, tape the coiled wire at one end onto the overhead projector (to prevent the wire from blowing away), and use a heat gun to straighten the wire. In a laboratory setting, students can do this experiment with their own strip of NiTi (see Experiment 10).

You may use resistive heating in lieu of hot air or water to demonstrate the shape-memory effect. For this experiment, connect a coiled NiTi wire to a 9-V battery with two alligator clips soldered to a 9-V battery snap. The current provided by the battery heats the NiTi and thereby transforms it back into the austenite phase. **CAUTION: Because of the large current drain, do not maintain the connection for more than 10 seconds. If the battery becomes hot, disconnect the wire immediately.**

Another twist on all of these experiments is to use a sample of NiTi that has been trained to spell "ICE" (Figure 9.1). After either crumpling the metal or stretching it to the point where it is no longer readable, the shape can be restored either by immersing it in water at about 50 °C, heating with hot air, or attaching alligator clips to the ends of the sample and connecting them to two 1.5-V dry cells hooked in series. A 6-V lantern battery will also work.

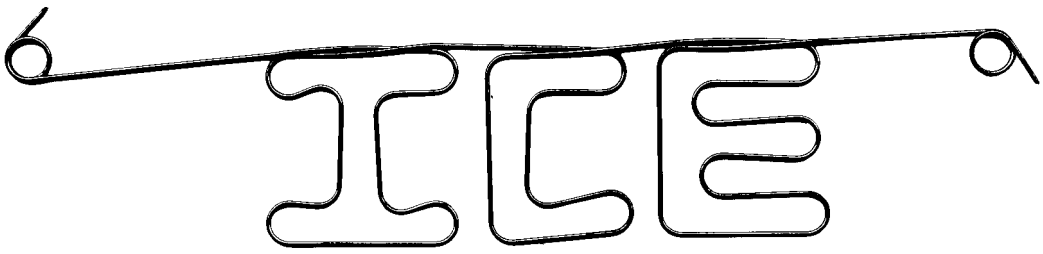

Figure 9.1. An illustration of the shape of a strand of memory metal that is trained to spell "ICE". (*See* Supplier Information.)

An understanding of the features of the shape-memory cycle lies in the relationship between the structures of the high- and low-temperature phases. These structures have been investigated in detail using X-ray diffraction (Chapter 4) *(11, 12)*. In Figure 9.2A the structure of austenite, the high-temperature phase, is shown from two different perspectives. The austenite phase adopts the CsCl structure (Chapter 5), shown at the

left, which can be described as having Ni atoms at each corner of the unit cell cubes and Ti atoms in the centers of the cubes, or vice versa. Smaller spheres lie behind the plane of the paper in this view.

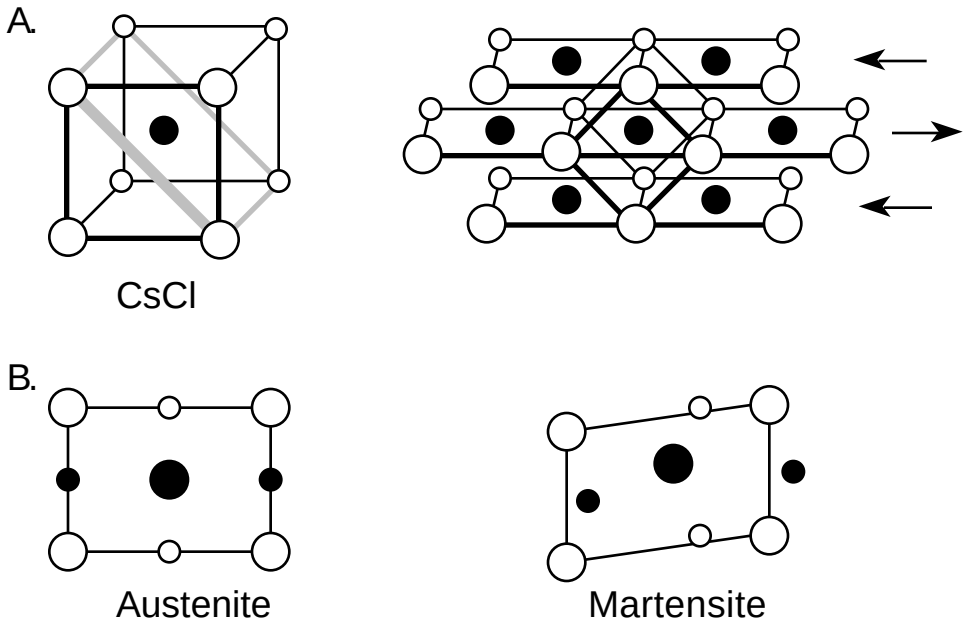

Figure 9.2. A: Two different views of the CsCl structure adopted by NiTi in the austenite phase. The common depiction is at the left, showing a cube of one type of atom with the other atom at the center of the cube. The white and black spheres represent the two kinds of atoms. The size of the spheres indicates depth; larger spheres are closer, and smaller spheres are farther away. At the right, the structure is depicted as series of stacked planes, with the cube also shown for comparison. The arrows indicate one component of the sliding of the planes that leads to changes in the atomic positions during the austenite-to-martensite phase transition. B: The structures of the austenite and martensite phases are represented by a two-dimensional projection of one of the rectangles shown in part A. Once again, the size of the spheres represents depth; the smaller spheres belong to the layer below the plane of the larger spheres. An additional shearing mechanism (not shown in A) also changes the angles in the structure of the martensite phase from 90 to 96°.

If the NiTi unit cell cube is balanced on a cube edge, the structure of austenite may also be represented as a stack of planes, as shown at the right in Figure 9.2A. This view is particularly useful in describing the relationship of the structure of austenite to the structure of martensite. As a more compact presentation of this view, the stack of planes can be reduced to a two-dimensional rectangular projection from above, with the rectangle derived from two edges and two face diagonals of the cubic unit cell (shaded outline at the left of Figure 9.2A). Two of the layers in the

stack are depicted in this manner at the left of Figure 9.2B: In this view, large spheres represent the atoms in the middle layer of Figure 9.2A, and small spheres represent the atoms in the next layer above or below.

During the structural transformation from austenite to martensite upon cooling, these particular planes of atoms in the austenite structure slide relative to one another (indicated by arrows on the right of Figure 9.2A), which does not change the 90° angles, and deform by shearing, which does change the 90° angles to about 96°. (A shearing motion, illustrated in Figure 9.3, can result when two opposing forces are displaced from one another.) Comparing the two-dimensional projection of the martensite with that of the austenite (Figure 9.2B) highlights the loss of 90° angles and the offset of alternating layers relative to one another as the austenite phase transforms into the low-temperature martensite phase.

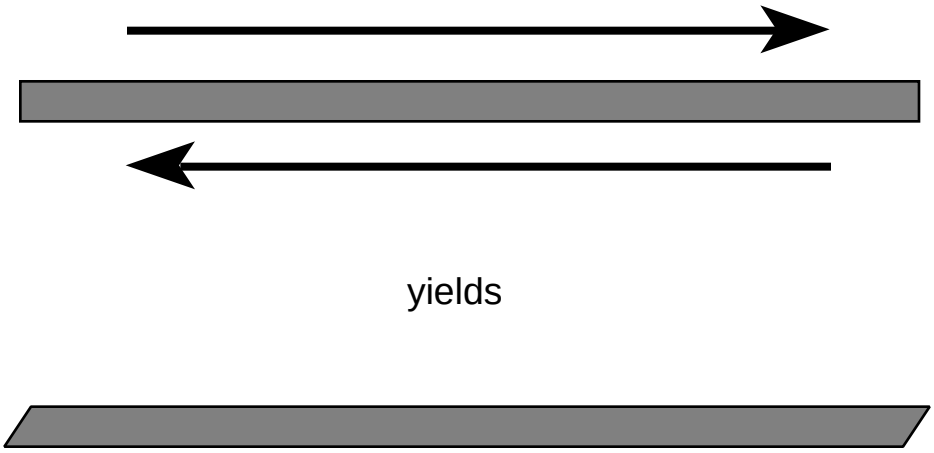

Figure 9.3. Application of displaced opposing parallel forces to an object creates shear.

Although the motions involved in the transformation from austenite to martensite are relatively simple, there are 24 different ways to carry out the transformation. To understand the origin of these 24 different so-called "variants," the directions of the two types of shearing during the transformation are shown in Figure 9.4A. The planes can shift relative to one another in each of two directions parallel to the face diagonal (marked by the dark arrows labeled a), and shear in each of two directions parallel to the cell edges (marked by pairs of arrows labeled b and c). In addition, there are six equivalent face diagonal planes in the CsCl structure, highlighted in Figure 9.4B. Each of these six sets of planes can thus shift in one of two directions and distort in one of two directions. The result is $6 \times 2 \times 2$ or 24 different ways to transform the structure into martensite.

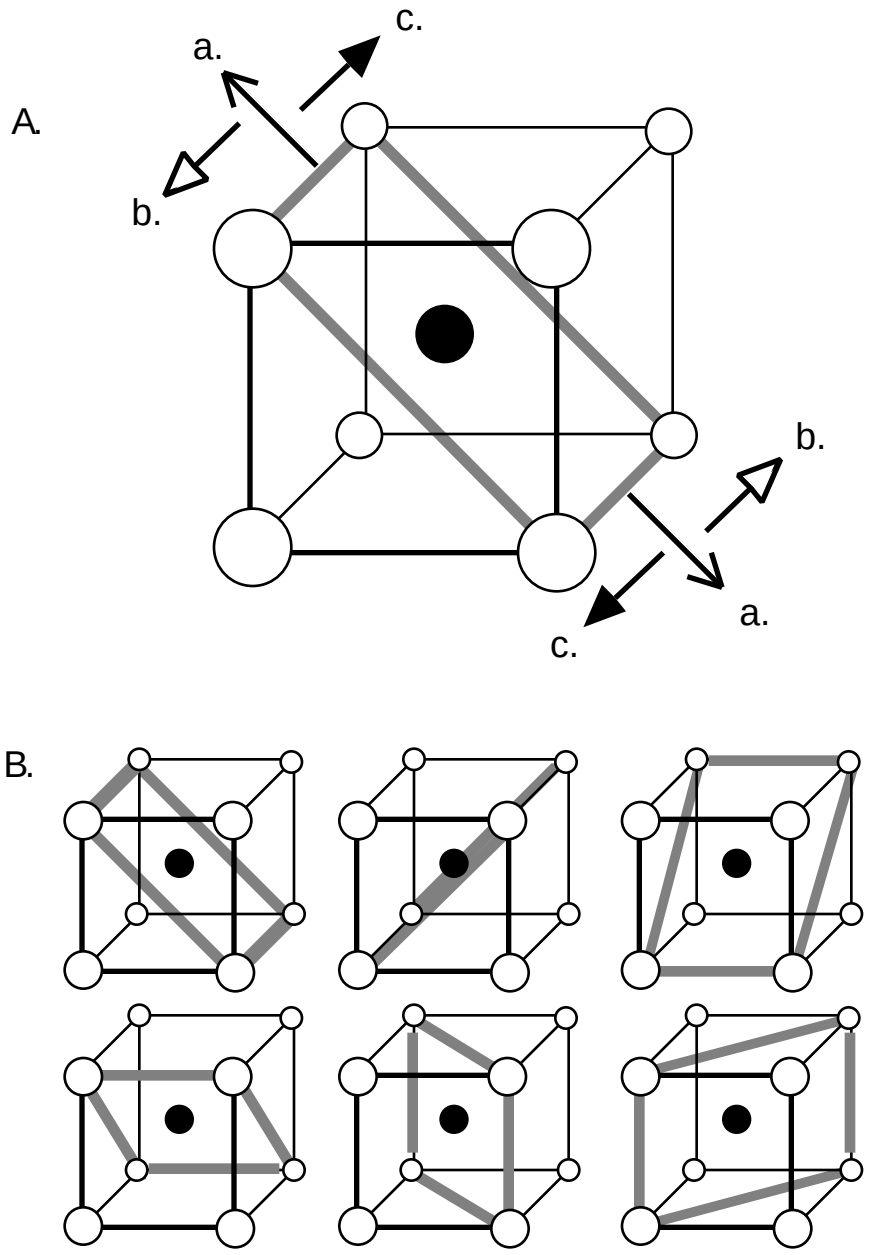

Figure 9.4. A: A total of four martensite variants may grow from each plane passing through a face diagonal in the CsCl structure. The planes may shift in the direction of either of the arrows labeled a at the edge of the face diagonal plane. This shifting will not change the 90° angles of the plane. An additional shear can occur through simultaneous motion in the directions indicated by either pair of arrows labeled b or c. These motions will destroy the 90° angles of the plane. B: Six equivalent planes pass through face diagonals in the CsCl structure. Thus a total of $6 \times 2 \times 2 = 24$ different variants may grow from the planes.

The phase transformation and shape-memory cycle is presented in Figure 9.5. At the top of the figure is the two-dimensional projection representation of the structure of austenite, a rectangle. The matrix of rectangles shown below this representation depicts how the structural units pack to fill space on a larger scale. As a sample of austenite is cooled through the phase-transition temperature, the structure transforms to martensite. To reflect the 24 different orientations of martensite, the variants, the long-range structure of martensite is represented in two dimensions in Figure 9.5 as a set of tilted parallelograms. These parallelograms can be packed together so that the overall shape does not change significantly during the phase change, and, as already noted, no observable change in shape accompanies the austenite-to-martensite transformation: The figure is meant to emphasize that the shape of the matrix of rectangles, and the matrix of tilted parallelograms on the atomic scale is roughly the same on the macroscopic scale. In fact, the density difference in the two phases is less than 0.5% (the martensite is slightly denser, discussed later) *(13)*.

The NiTi wire, as purchased, is typically in the low-temperature martensite phase at room temperature. The wire has been previously trained to remember a linear shape in the austenite phase. When the NiTi is bent or coiled in the low-temperature martensite phase, the effect on the microstructure is a reorientation of the variants corresponding to a macroscopic change in shape. This reorientation is shown in the lower left of Figure 9.5, as the inclination of most of the parallelograms to a common direction. This reversible mechanism for accommodating stress distinguishes NiTi from most metals, in which similar stress would introduce defects into the crystal structure, or cause planes of atoms to slip past each other and permanently deform the metal.[3]

In the last step of the shape-memory cycle, heat is used to transform the martensite back into the austenite phase. The atoms recover their initial positions, and the initial macroscopic shape of the sample is restored. Although several pathways back to the austenite structure exist, only the lowest energy pathway restores the initial ordered CsCl structure in which Ni atoms are surrounded exclusively by Ti atoms and vice versa. Other paths would produce higher energy structures in which Ni and Ti atoms have a mixture of Ni and Ti atoms as nearest neighbors in the crystal.

The enthalpy associated with the phase change is relatively small, as is typical for a solid-state phase transformation: The conversion of austenite to martensite is modestly exothermic with an enthalpy change on the order of only –2 kJ/mol.

---

[3]Bending a metal can result in work hardening. *See* Chapter 6.

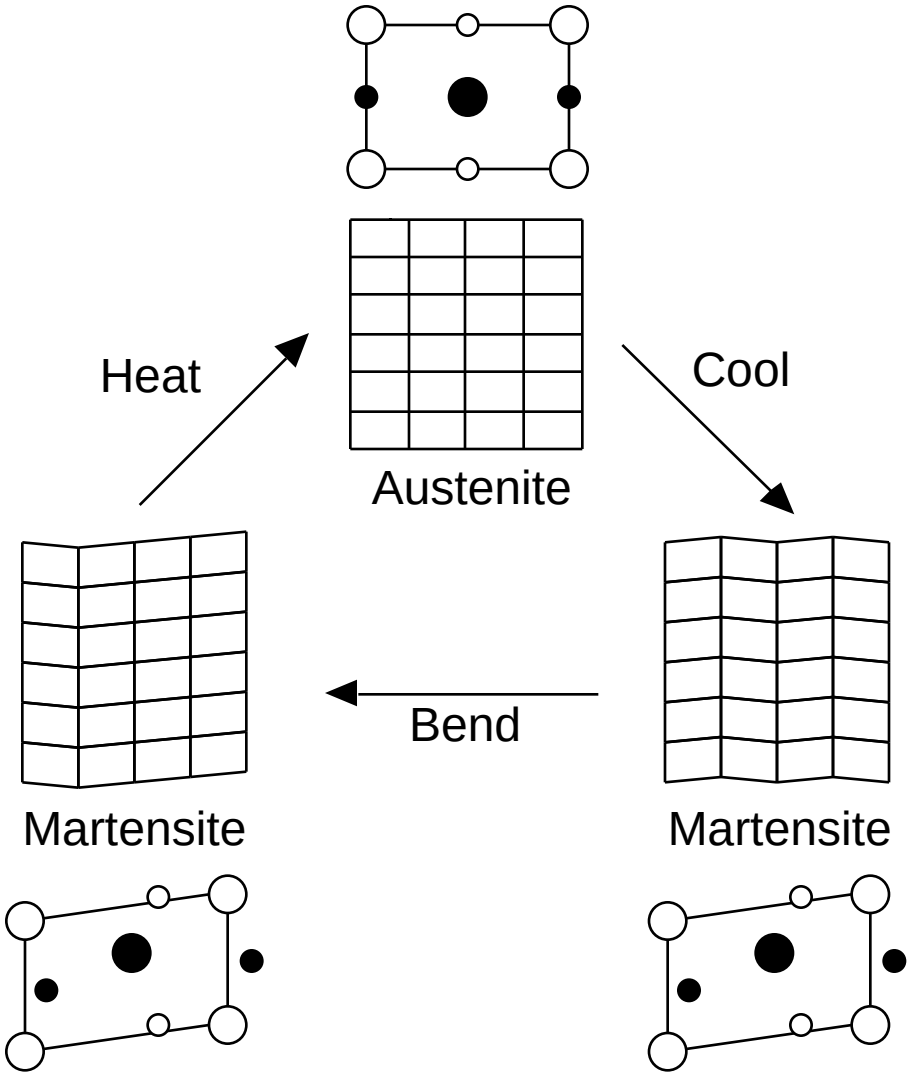

Figure 9.5. The structural features of NiTi that give rise to the shape-memory effect. The cycle starts with the NiTi in the austenite phase shown at the top of the figure. As the NiTi is cooled, going clockwise around the cycle, the transformation into the martensite proceeds. The diagonal planes slide past each other (as shown in the upper right of Figure 9.2A) and deform slightly to a parallelogram in the two-dimensional projection. In this projection, two differently oriented martensite variants, one angled to the left and one to the right, may be observed. When the martensite is bent, the variants can reorient from left to right or vice versa to relieve the stress. When the NiTi is heated, the lowest energy pathway returns the atoms to their original positions and maintains the ordering of the atoms, with nickel atoms surrounded exclusively by titanium atoms and vice versa.

Changing the "Memorized" Shape of NiTi

As purchased, samples of NiTi are polycrystalline, meaning that regions of crystallinity on the order of micrometers in size (occasionally as large as a millimeter) are separated from one another by grain boundaries (Chapter 6). Within the grains, the nickel and titanium atoms are arranged with almost perfect order. However, occasional mistakes in the packing, such as dislocations and other defects described in Chapter 6, may occur *(14)*. The nickel and titanium atoms must return to exactly the same position each time the NiTi is heated into the austenite phase, so the configuration of defects in this phase effectively pins the austenite into a given shape. To give the NiTi a new shape to remember requires substantial energy, provided, for example, by heating the NiTi in a candle flame to about 500 °C, while it is physically held in the desired shape. During the annealing (heating) process, the atoms surrounding the defects gain enough energy to relax into lower energy configurations, and this new configuration of defects effectively pins the austenite into its new shape. The gentle heating used in the shape-memory demonstration to return to the austenite phase from the martensite phase does not provide enough energy to allow the defects to readjust.

Demonstration 9.3. The Annealing of NiTi into a New Shape

Materials

NiTi wire (3 inches long, 0.03-inch diameter; *see* Supplier Information)
Candle and matches
Heat gun or hot water

Procedure

- Grasp the two ends of the wire, and place the middle of the wire in the center of the candle flame. Try to bend the wire into a V-shape. It will yield as it becomes hot, at which point it should be removed immediately from the flame.
- The wire will cool off in a few seconds by waving it in the air or blowing on it. After the wire has returned to room temperature, Demonstration 9.2 can be repeated: The wire can be coiled, but upon heating with hot water or the heat gun, it will now return to the V-shape, not the linear shape.

More complicated shapes like the "ICE" sample described in Demonstration 9.2 require a jig like that shown in Figure 9.6, because the heat treatment will initially cause the wire to try to recover its original shape before it relaxes into the new shape. The jig itself consists of a series of metal pegs firmly mounted in a metal base. The wire is wound tightly around the pegs and fastened securely at either end. The

apparatus is placed in a standard box furnace for about 15 minutes at 500–540 °C. Prolonged heating should be avoided as that seems to degrade the shape-memory behavior. Again, these are the conditions that have been used to prepare the "ICE" sample; the preparation of samples such as this with fairly complicated shapes is very sensitive to temperature, oven geometry, and heating time. The conditions described here may have to be modified to form other shapes.

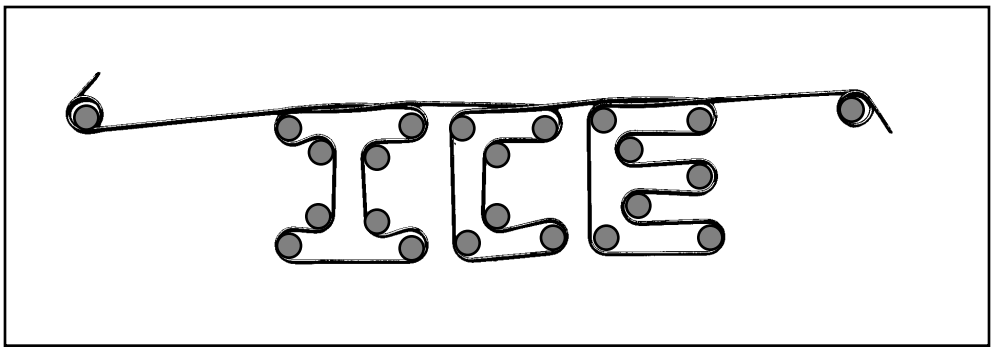

Figure 9.6. The jig used to train the memory metal that spells "ICE".

Mechanical Properties and Superelasticity of NiTi: Changing Phase with Pressure

The different structures of austenite and martensite result in considerably different mechanical properties for the two phases. The CsCl austenite structure is relatively rigid and hard. In contrast, the ability to re-orient variants of the martensite phase imparts mechanical flexibility and makes the low-temperature phase a little softer than the high-temperature phase.

Although the structural cycle just discussed is based on using temperature to interconvert the two phases of NiTi, the equilibrium is also a strong function of pressure. Under certain conditions, the austenite phase may be mechanically transformed into the martensite phase, and become elastic; that is, when the stress is removed, the martensite phase will transform back to the austenite phase and the NiTi will return to its undeformed shape. This mechanical property is sometimes known as "pseudoelasticity,"[4] or more specifically "superelasticity," and many NiTi applications are based on it.

Superelasticity may be understood as another example of the pressure-induced phase transformations discussed at the beginning of this chapter. Applying mechanical pressure to NiTi in the austenite form can cause the transformation to martensite to occur without a change in temperature.

---

[4]It is pseudoelasticity and not elasticity because the strain, or fractional change in length of the wire under tension or compression, is not quite linear with the amount of tension or compression that is applied.

This mechanically induced pressure, called stress, is a force exerted over an area of the material, and thus has units of pressure. Both tensile stress, in which the atoms are pulled apart (by applying tension), and compressive stress, in which the atoms are pushed together (by compression), can occur when a material is bent, as shown in Figure 9.7.

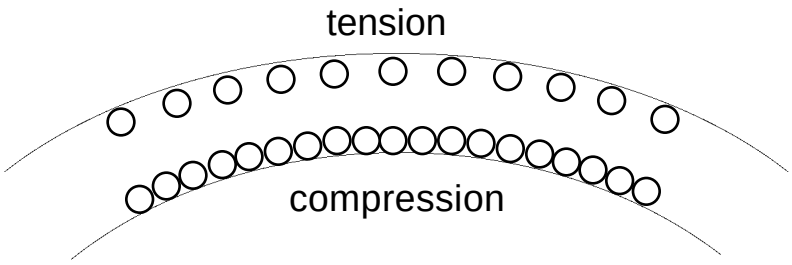

Figure 9.7. The simultaneous occurrence of tension (atoms are pulled apart) and compression (atoms are pushed together) when a metal rod is bent.

The conversion under pressure of the lower density, austenite structure to the higher density, martensite structure is analogous to the transformation under pressure of low-density, gaseous water to the denser, liquid form of water. In accord with the prediction of Le Chatelier's principle, application of pressure will favor formation of the denser martensite phase (*see* Figure 9.8), even though the difference in densities of the two phases is less than 0.5%.

Another way to visualize this relationship is with the traditional phase diagram for water that is shown in most general chemistry texts. On the pressure–temperature phase diagram, lines with positive slopes (like that representing the gas–liquid water equilibrium) indicate that an increase in pressure at a given temperature will raise the temperature at which interconversion of the two phases occurs (the boiling point, for example), and thus permit conversion of some of the gas to the liquid state. The Clapeyron equation can be used to quantify the effect.[5] Similarly, bending a sample of NiTi in the austenite form will cause an increase in the characteristic temperature at which the sample begins to be converted into the martensite phase in the region of the solid that is being compressed by the bending motion. If the increase in this temperature is large enough, calculable with the Clapeyron equation, some of the austenite will be converted to martensite. Releasing the stress causes the martensite to transform back into austenite with restoration of the original shape.

---

[5]In the case of the martensite–austenite transformation, a modified form of the Clapeyron equation may be used to determine the change in the martensite start temperature, M_S (the temperature at which the sample begins to transform into martensite; Figure 9.9), based on the applied stress, σ, and the strain, ε (the fractional change in length): $d\sigma/dM_S = -\Delta H/T\varepsilon$. The analogous equation in terms of pressure and volume changes is $dP/dT = \Delta H/T\Delta V$.

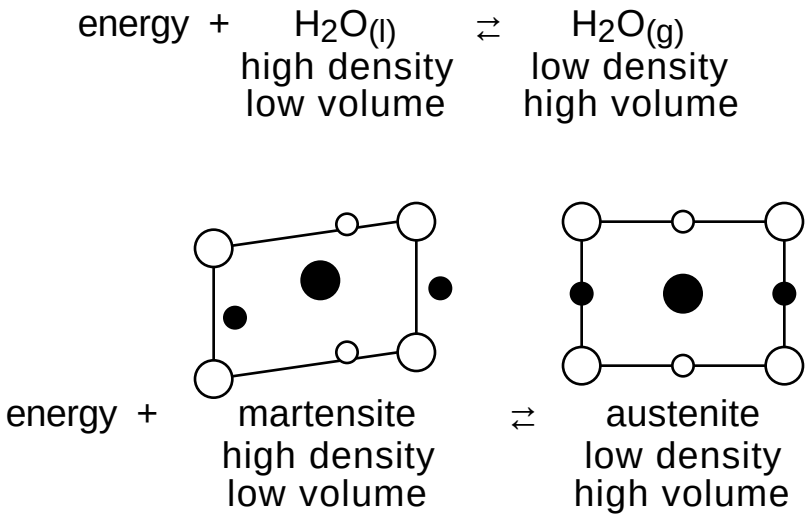

Figure 9.8. The application of pressure will cause the austenite form of NiTi to transform into martensite at temperatures higher than those at which the transformation would occur at ambient pressure. This behavior is analogous to the observation that the boiling point of water rises under conditions of applied uniform pressure.

Thicker NiTi rods can be used to illustrate the critical role that atomic structure plays in defining mechanical properties.

Demonstration 9.4. The Mechanical Properties of Two NiTi Phases

Materials

NiTi rods (Shape Memory Applications; see Supplier Information) Rods of differing stoichiometry (2.5 inches long by 0.10 inch in diameter) are available in both the low-temperature (martensitic rods) and high-temperature phase (austenitic rods) at room temperature. The rods have slightly different Ni:Ti atomic ratios, leading to different temperatures for the phase transition, as will be discussed *(15)*.
Hot water (above 50 °C)
Liquid nitrogen in a 1-L Dewar flask
Tongs
Gloves
Heat gun
Overhead projector and screen (optional)

Procedure

- Try to bend rods that are in the two different phases at room temperature. A rod that is in the high-temperature austenite phase at room temperature will be extremely difficult to bend into a V-shape. In contrast, a rod that is in the low-temperature martensite phase at room temperature is comparatively flexible. Of course, the bent rod can be placed in very hot water (above 50 °C) or in front of a heat gun to restore its linear shape.
- Cool an inflexible rod that is *in the austenite phase at room temperature* in liquid nitrogen. **CAUTION: Liquid nitrogen is extremely cold. Do not allow it to come into contact with skin or clothing, as severe frostbite may result. Wear gloves when transferring and using liquid nitrogen.**
- Use tongs to remove the rod from the liquid nitrogen. While wearing gloves, bend it into a V-shape. As the rod warms back to room temperature, it will return to a linear shape. (The bent rod can be placed on an overhead projector to show its return to linearity to an audience.)
- Alternatively, immerse a rod that is in the martensite phase at room temperature in very hot water. It will become inflexible when hot and flexible as it cools back into the martensite phase.
- Try to scratch a rod in the martensite phase with one in the austenite phase. The end of an austenitic rod will scratch the martensite, but a martensitic rod will not scratch the surface of the austenite. This activity demonstrates the hardness of the austenite compared to the martensite.

Superelasticity can be demonstrated with a pair of eyeglasses having frames made from NiTi memory metal. The NiTi must start in the austenite phase for this application; therefore, the transition temperature must be set slightly below room temperature.

Demonstration 9.5. Superelasticity

Materials

Eyeglass frames made from NiTi memory metal (commonly available from optometrists)
Overhead projector
Liquid nitrogen and Dewar flask with a large enough mouth to accommodate the frames
Gloves
Tongs

Procedure

- Lay the eyeglass frames on the overhead projector to show the initial shape.
- Bend the frames. When bent, the frames yield. But once the stress is released, the frames snap back into their original shape.
- Cool the frames in liquid nitrogen. **CAUTION: Liquid nitrogen is extremely cold. Do not allow it to come into contact with skin or clothing, as severe frostbite may result. Wear gloves when transferring and using liquid nitrogen.** Allow them to remain there until thermal equilibrium is reached.
- Put on insulating gloves and remove the frames from the liquid nitrogen using the tongs. Bend the frames. Lay the bent frames on the bench top or on an overhead projector. Observe what happens as the eyeglasses return to room temperature. The frames stay bent if bent when cold, but return to their original shape on warming to room temperature.

Acoustic Properties of NiTi Phases

The structural differences between austenitic and martensitic NiTi affect sound propagation in the two forms of the solid. The regular structure of the austenite leads to a ringing sound when a sample is dropped or struck: a sound wave launched in the material travels relatively unimpeded through it. In the martensite phase, the boundaries between regions with different orientations (the variants) appear to act as baffles for vibrations, resulting in a more muffled-sounding thud when martensitic samples are dropped.[6] Cold-worked metals, which have a very high density of induced defects, are very good at absorbing sound.

Laboratory. The marked acoustical difference in the two phases also permits students to determine the approximate temperature of the phase transformation for the NiTi rods. A laboratory procedure is given in Experiment 10.

[6]Above about 20 K, defects in metals are the primary absorbers of sound waves traveling through metals, and boundaries between martensitic variants behave similarly. *See* reference 16.

Demonstration 9.6. Acoustic Properties of Two NiTi Phases

Materials

NiTi rods (one austenitic and one martensitic; 0.10-inch diameter, 2.5 inches long; *see* Supplier Information)
String
Stirring hot plate and stirring bar
400-mL beaker
Water
Thermometer
Ring stand and ring

Procedure

- Tie a string around a rod that is in the martensite phase at room temperature.
- Fill the 400-mL beaker with water and place it on the stirring hot plate. Add a stirring bar and begin stirring but not heating.
- Loosely tie the string to the ring of the ring stand and suspend the rod in the water so that it is not touching the side or the bottom of the beaker but is completely submerged.
- After the rod has been immersed for about 2 minutes, record the temperature of the water, untie the string from the ringstand, and immediately drop the rod onto a solid surface such as a benchtop or a cement floor. Note the sound that the rod makes when dropped (thud, ring, or intermediate).
- Return the sample of nitinol back to the water bath and begin slowly heating it. The hot plate should be on the lowest setting. Remove the rod from the water bath at 10 °C intervals and drop it, recording the sound made upon dropping the sample until it is clearly in the high-temperature phase. (A clear ring will be heard. This sound can be verified by dropping the austenite rod.)
- The characteristic acoustic signatures of the two phases of NiTi are revealed simply by dropping them. The austenite rods will ring like a bell, and the martensite samples will yield a dull thud! A sample that contains both phases (discussed later) will yield a sound that is intermediate between a ring and a thud. For best results, the rod should be dropped from a roughly reproducible initial position that is approximately parallel to the surface it will strike, and from a height that ensures an easily recognizable sound. The audio characteristics can also be measured as the bath cools back to room temperature.

Hysteresis

More quantitative measurements of the phase change in NiTi, through magnetic, electrical, calorimetric, or diffraction measurements, reveal that the heating curve may be displaced toward higher temperature from the cooling curve, as shown in Figure 9.9, a phenomenon known as hysteresis. Hysteresis reflects the fact that one solid phase needs to grow within a region of the other. Growth of the new phase creates elastic strain in the crystalline region around it, adding to the chemical free energy necessary for enlarging the grain of the new phase *(8, 17)*. Thus, no matter how slowly the conversion takes place, this thermodynamically based displacement of the heating and cooling curves will occur, although it may be very small.

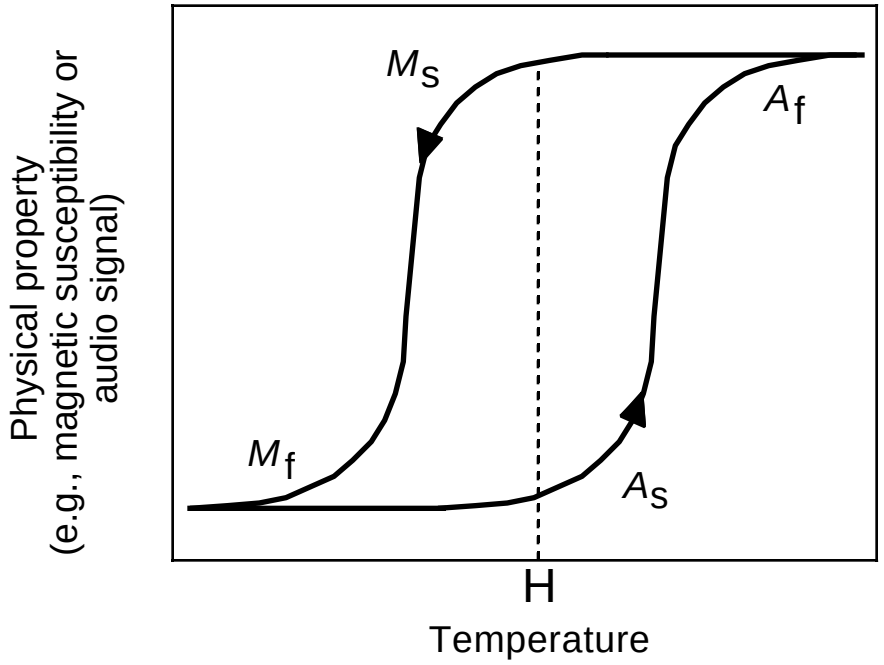

Figure 9.9. The martensitic phase transformation in NiTi is evident in a number of physical properties. For example, the general characteristics of the magnetic susceptibility as a function of temperature show four transition temperatures: A_s, the start of the martensite-to-austenite transition on heating; A_f, the end of the martensite-to-austenite transition on heating; M_s, the start of the austenite-to-martensite transition on cooling; and M_f, the end of the austenite-to-martensite transition on cooling. The heating and cooling curves are often separated by as much as 20 °C. This separation, or hysteresis, allows both the austenite and martensite to be accessible at the same temperature (marked H), depending upon whether the sample was previously heated or cooled.

The rods used to investigate the acoustic properties of the two phases may or may not exhibit hysteresis in the experiment. With some NiTi samples, an intermediate phase may grow during the austenite-to-martensite transition, the so-called R (rhombohedral) phase, which may show relatively little hysteresis in its conversions with austenite *(9, 18)*. Any samples that are found to have a significant displacement in the heating and cooling curves lend themselves to the following interesting experiment: At certain temperatures in the middle of the transition region, such as the one labeled H in Figure 9.9, the sample will thud if it is first cooled into the martensite phase, then heated to temperature H and dropped. In contrast, if the sample is first heated into the austenite phase, then cooled in the bath to temperature H and dropped, it will ring. That is, the sample phase(s) present at temperatures within the hysteresis loop depend on the thermal treatment used to reach the temperature.

Chemical Composition

NiTi has been prepared traditionally by heating the elements together above the NiTi melting point (1200–1300 °C, depending on composition). Exclusion of oxygen is critical during the synthesis because of the ease with which Ti oxidizes.

NiTi can tolerate small deviations in chemical composition around the 1:1 stoichiometry before the shape memory effect is lost. A more accurate representation of NiTi within this range is Ni_xTi_{1-x}, wherein the shape-memory effect has been observed when x lies between 0.47 and 0.51. However, the temperature at which the martensitic phase change occurs in NiTi is a sensitive function of stoichiometry. As indicated in Figure 9.10, variations of a few percent around the equiatomic point in Ni_xTi_{1-x} cause substantial changes in the temperature of the phase transformation *(15)*.

One of the reasons that the transition temperature begins to fall with increasing Ni content is that small domains of other phases begin to precipitate as the composition deviates from 1:1 (x = 0.50). In addition, small quantities of impurity atoms that may be present may also influence the transition temperature. Tuning of the transition temperature to as high as several hundred degrees has been accomplished by partial or complete substitution of Ni with Pd or Pt *(19, 20)*. Conversely, substitution of Ni with a few percent of Co or Fe substantially reduces the transition temperature. A discussion of the effects of adding a third transition metal may be found in reference 21. The result of this strong dependence of transition temperature upon composition is that samples of memory metal (such as the rods used in the demonstrations) can be made in either the martensite or the austenite phase at room temperature.

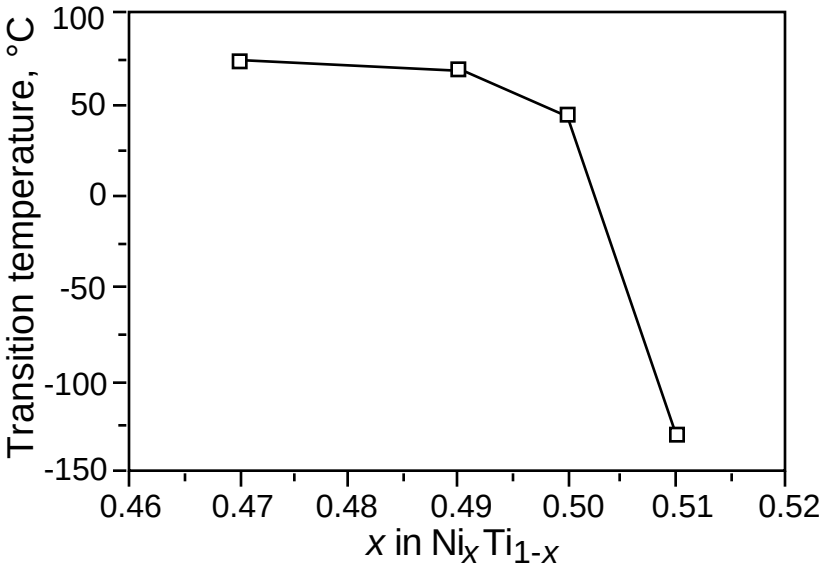

Figure 9.10. The effect of nickel concentration on the temperature of the phase transition. (Adapted from reference 18. This is a compilation of data by several researchers, who measured the composition and transition temperatures by different methods.)

Applications

Shape-memory alloys have been incorporated into a wide variety of applications. An overview of recent applications using shape-memory alloys may be found in reference 22. Some creative suggestions from undergraduates at the University of Wisconsin—Madison are presented in the following list. The shape-memory effect creates a temperature-sensitive "on–off" switch that has been used in coffee makers and scald-proof shower heads. Diesel-fueled Mercedes Benz cars have a shape-memory alloy-based valve that regulates the flow of transmission fluid in the engine as a function of temperature *(23).* The NiTi memory metal valve controls the shifting pressure in the automatic transmission (as the temperature in the engine goes up, a higher pressure is desirable), and this pressure control in turn smoothes shifting between gears.

As shown in Figure 9.11, one NiTi spring, one steel spring, and a piston provide the switching mechanism. The springs and the piston are housed in a case with an inlet and outlet at the top and bottom. When the engine is cold, the NiTi spring is in the martensite phase, and is flexible. The steel spring provides enough force to push the piston to the left and collapse the NiTi spring. This collapse closes the flow path through the valve. As the engine warms up, the NiTi transforms into the austenite phase and remembers its expanded shape. It pushes against the piston and the steel spring, opens up the valve, and allows oil to flow through. If the NiTi is not strongly deformed, it can be switched through millions of cycles.

Suggested Uses of NiTi
Fishing hook—straightens when heated for easy removal
For spies—send ordinary looking wire, pop in hot water for message
Siding and roofing on houses—sun repairs baseball damage
Cookware—heating repairs dents
Meat thermometer—sticks out when done
Jewelry
Clamps and locks
Fire detectors
Safety device for household irons
Wind chimes made from austenitic rods
Malleable “Chemistry Action Figures” made from the martensite form
Moving sculpture
Levers

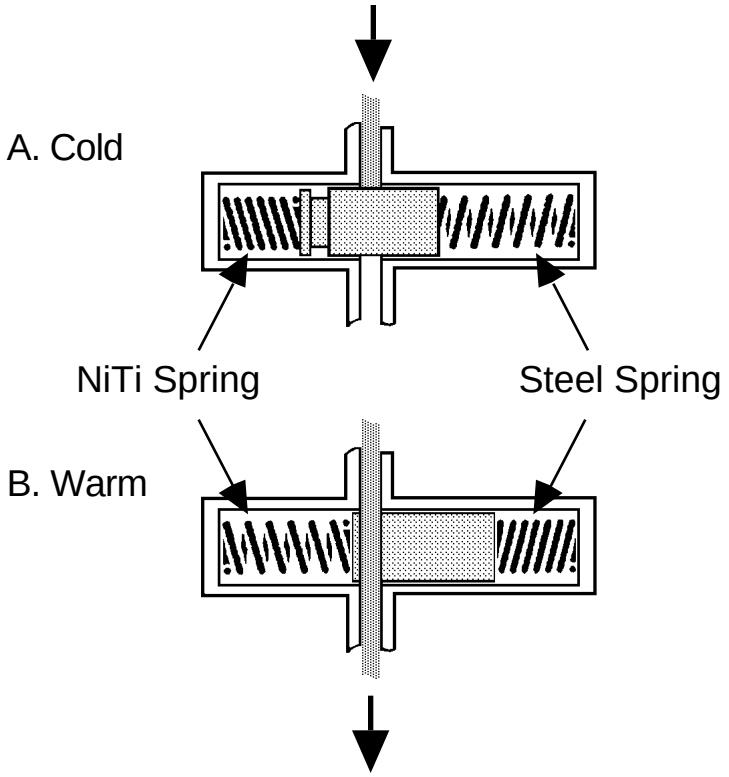

Figure 9.11. NiTi-actuated governor valve for automatic transmissions. The steel spring easily compresses the memory metal spring when it is in the low-temperature martensite phase. As the temperature increases, the NiTi spring remembers its extended shape (it transforms into the austenite phase) and becomes rigid, and thus forces the steel spring to compress. This compressed spring opens the pathway for transmission fluid through the valve. (Reprinted with permission from reference 23. Copyright 1991.)

NiTi has been used to create sculptures with moving parts. Olivier Deschamps designed the sculpture entitled "Les Trois Mains" (The Three Hands) *(24)*. When the weather is cool, the NiTi hands are in the martensite phase, and the hands are pointed down toward the center of the sculpture. If the day is warm, the NiTi transforms into the austenite phase, and the hands reach upward. Similarly, a sculpture by the same artist entitled "Espoir–Desespoir" (Hope–Despair) shows a kneeling woman with a baby on the ground in the martensite phase; upon warming, the sculpture is transformed so that the woman lifts the baby toward the sky. (Figure 9.12). An intriguing idea is to make automobile bumpers out of memory metal: The effects of an accident could be reversed simply by heating the car!

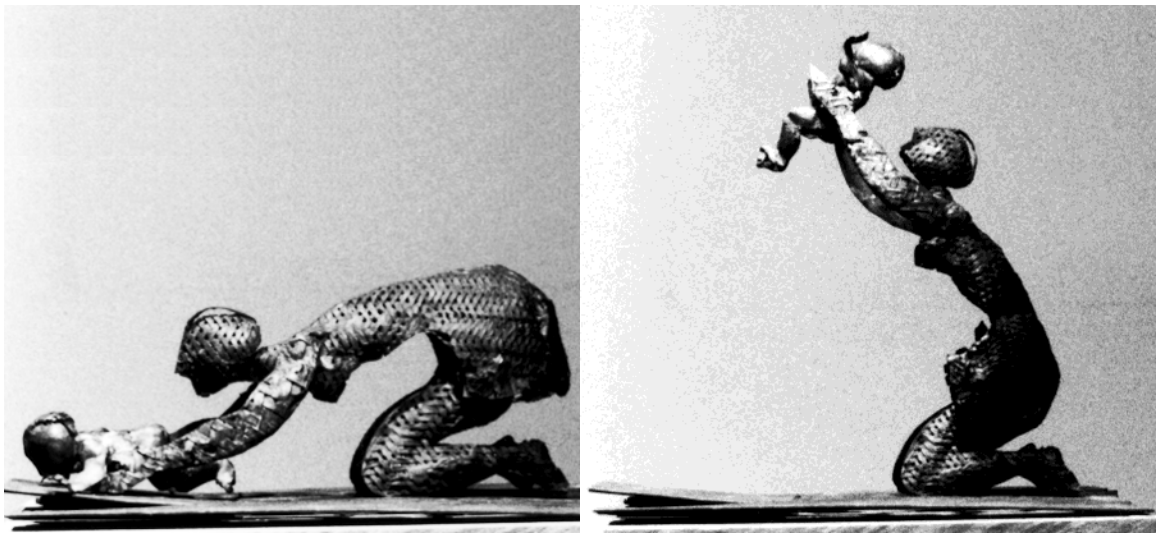

Figure 9.12. The sculpture "Espoir-Desespoir" (Hope-Despair) by Olivier Deschamps shows a kneeling woman with a baby on the ground (left photo; NiTi is in the martensite phase). Upon warming, the sculpture is transformed (NiTi is then in the austenite phase) so that the woman lifts the baby toward the sky (right photo). (Photographs courtesy of Olivier Deschamps, Paris, France.)

The most common use of NiTi is in biomedical applications for which its combination of strength, flexibility, and biocompatibility is desirable. The pseudoelastic property of NiTi is used in orthodontic braces. To straighten teeth, an "archwire" is connected across each tooth by a brace. The archwire is pulled tight, and this aligns the teeth. If a NiTi archwire in the austenite phase is used, the stress from tightening causes it to transform into the martensite phase. After tightening, the force the wire exerts as it tries to return to the austenite gradually pulls the teeth into position. The advantage of NiTi is that the wire can be pulled tighter than other types of wire, and therefore fewer trips to the orthodontist are needed. Because the force comes from the phase transformation, it is more even and continuous over time than the force from other types of wire, which tend to pull a lot at first, and then relax. Other biomedical

applications for NiTi include staples that use body heat to cause the phase transformation and clamp broken bones together, and guidewires for arthroscopic surgery that are strong but flexible.

The 1-2-3 Superconductor

Superconductivity owes its discovery to a Dutch physicist, Heike Kamerlingh Onnes. In the early 1900s, Kamerlingh Onnes accomplished the then remarkable feat of liquefying helium. The ability to drop temperatures to a few kelvins (helium boils at 4.2 K at atmospheric pressure) suddenly opened a larger window for studies of thermal effects. Kamerlingh Onnes exploited his new tool by measuring the electrical resistance of metals at these very low temperatures. In 1911, while measuring the resistance of mercury, he found an astonishing result: at about 4 K, the resistivity abruptly dropped below his ability to measure it. Nor was mercury unique in displaying what appeared to be zero resistance to a flow of electrical current. Several other metallic elements exhibited the same effect at temperatures of a few kelvins. This remarkable electrical property was treated as a diagnostic for a new state of matter, the superconducting state. The temperature below which the material becomes a superconductor (this represents a kind of phase change; discussed later) is called the critical temperature, T_c. *(25)*

About 20 years later, in 1933, another surprising characteristic of superconductivity was discovered by W. Meissner and R. Ochsenfeld. They found that a superconducting material will not permit a magnetic field to penetrate its bulk, a property that has come to be called the Meissner effect.

These two diagnostics of superconductivity, resistanceless current flow and perfect diamagnetism, were appreciated even many years ago as having tremendous technological implications. But two major obstacles to implementing any new technology existed. First, extremely cold temperatures were required to achieve the superconducting state. Although liquid helium could serve as a coolant, its scarcity and processing costs made it expensive; moreover, sophisticated equipment was required to handle it. The second problem was that the superconducting state of these elemental metals was easily destroyed by the application of modest external magnetic fields or electrical transport currents; thus their use in electromagnetic applications was impractical.

These problems prompted an intensive search for new materials that would become superconducting at higher temperatures and retain their superconductivity in the presence of large magnetic fields and electrical currents. In particular, scientists who studied this phenomenon dreamed of achieving superconductivity at or above 77 K (–196 °C), in which case liquid nitrogen (boiling point, 77 K), which is cheaper and more easily handled, could be used as a coolant.

Until recently, alloys of niobium, particularly Nb–Ti, had been responsible for the greatest advances in superconductor technology. Their ability to remain in the superconducting state while supporting large electrical currents led to limited but extremely important applications such as the construction of powerful electromagnets. In 1973, superconductivity with Nb_3Ge was observed at 23 K, which until 1986 was the highest observed T_c value. Another breakthrough involved the observation of superconductivity with certain organic salts, whose structures feature one-dimensional stacks of organic moieties that can be modified by chemical substitution. These salts have required liquid-helium-range temperatures to become superconducting.

In spite of these advances, there was no evidence of superconductivity at temperatures anywhere near 77 K, even after some 70 years of investigation: More than 20 metallic elements had been found to exhibit superconductivity (Figure 9.13), but they did so only at very low temperatures near that of liquid helium *(26)*. Furthermore, most of the simple alloys or compounds based on combining two or three elements also required disappointingly low temperatures for superconductivity.

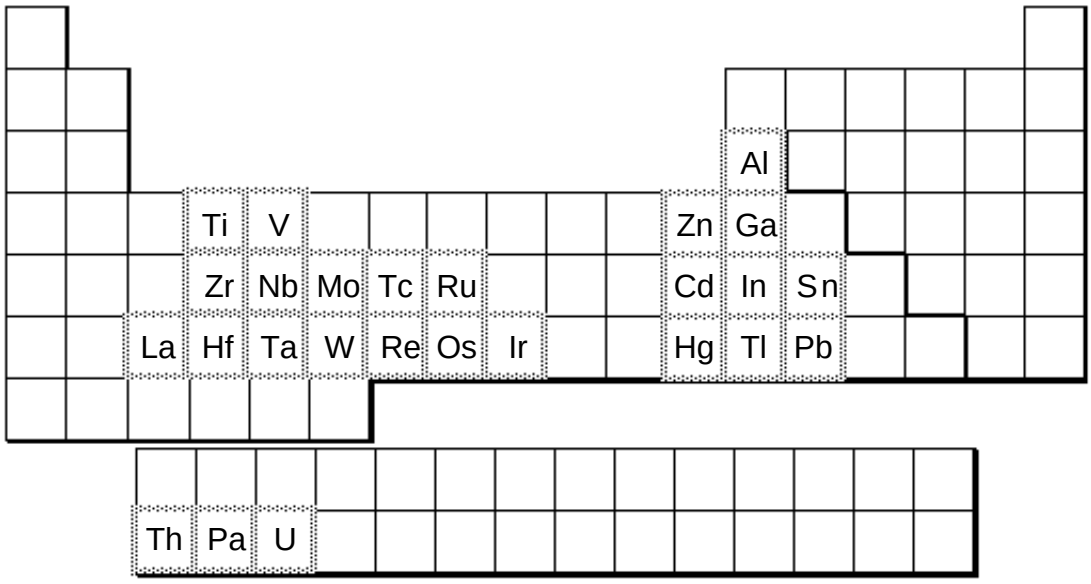

Figure 9.13. The periodic table, with elements that exhibit superconductivity at ambient pressure indicated by outlined boxes. All of these elements require temperatures of less than 10 K to attain the superconducting state *(26)*.

It was against this setting that two scientists working at the IBM facility in Zurich, Georg Bednorz and K. Alex Müller, reported a startling result in early 1986: A ceramic oxide of lanthanum, barium, and copper lost its resistance at about 30 K *(27)*. That a metallic oxide should not only exhibit superconductivity but do so at such a high temperature struck many in the scientific community as incredible. Suddenly a whole new

family of materials, ceramics, was ripe for investigation, and the pace of research accelerated markedly.

In 1987, groups at the University of Houston and University of Alabama, headed by Paul Chu and M. K. Wu, Jr., respectively, announced the discovery of a related oxide that was superconducting above 77 K. This material was later determined to have the formula $YBa_2Cu_3O_{7-x}$ (commonly called "1-2-3" because of the Y:Ba:Cu atomic ratio) *(28, 29).* Part of the charm of this high-tech material is its relative ease of preparation. Superconductivity at the temperature of liquid nitrogen is now commonplace, and efforts continue to find materials that can push superconductivity up toward room temperature. At present, however, much of the focus of research has shifted from increasing T_c to increasing the critical current density (the current density above which superconductivity is lost, often reported in amperes per square centimeter) and making the materials in usable forms such as thin films and wires.

Laboratory. Experiment 11 describes the synthesis and explores the properties of the 1-2-3 superconductor.

Physical Properties of Superconductors

To appreciate the phenomenon of superconductivity, some of its physical and chemical characteristics will be described in more detail, along with some applications.

Loss of Resistance

A material's passage into the superconducting state is characterized by an abrupt change in its resistivity as it is cooled. As noted in Chapter 7, in ordinary conducting materials the flowing electrons that represent current always encounter some resistance, which can be likened to friction. The source of the resistance is the scattering of electrons from the atoms that make up the conducting material. Scattering arises from the defects (Chapter 6) and from the vibrations of the atoms in the solid. Ohm's law relates the current, I, to the voltage, V (the difference in electrical potential between points in a circuit that causes electrons to flow), and resistance, R, thus: $V = IR$.

Figure 9.14 graphs the resistivity of a superconducting material (the resistance is proportional to resistivity) as a function of temperature. As the sample is cooled, there is initially a smooth decline in resistivity with temperature; with less thermal energy available, the atoms vibrate less, and less scattering results. In a normal metal (Chapter 7), this decline ceases at very low temperatures when scattering becomes limited by

fixed defects; a limiting or residual resistivity exists. What characterizes the superconducting state, however, is a sudden drop to zero resistivity at the critical temperature, T_c. Below T_c, a direct current can flow indefinitely in the material so far as anyone has been able to determine.

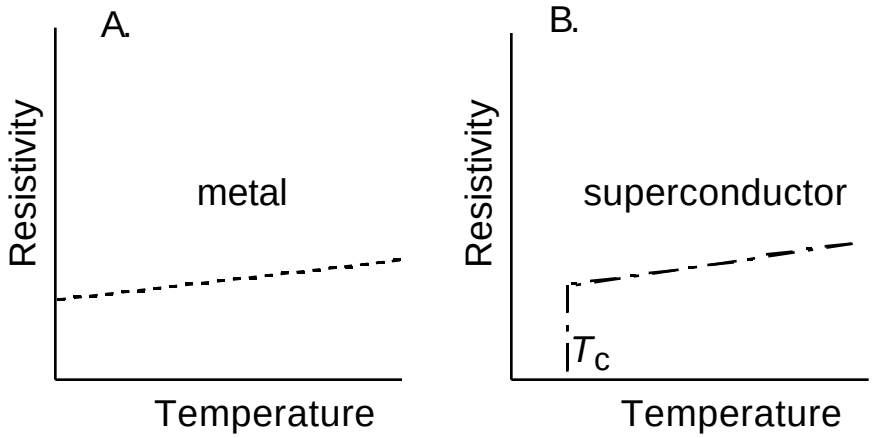

Figure 9.14. Resistivity as a function of temperature for (A) a metal and (B) a superconductor.

The transition from a normal metal to a superconductor can be regarded as a so-called "second-order" phase change. Unlike the phase change associated with the conversion of a liquid to a gas, the enthalpy of the phase change is zero, but there is a change in the specific heat of the material.

The Meissner Effect and Levitation

Besides resistanceless current flow, the other characteristic of a superconducting material is that it is perfectly diamagnetic. The expulsion of magnetic field lines from the interior of a material as it passes from the normal to the superconducting state at T_c is illustrated in Figure 9.15.

This description applies to so-called "Type I superconductors," the class to which many of the early superconductors belong. For "Type II superconductors," which include the ceramic, high-temperature superconductors like 1-2-3, it is only partially correct: At low magnetic field strengths the magnetic field is completely expelled from the superconductor's interior; however, as the magnetic field strength increases, more and more magnetic field lines enter the solid (they do so in a pattern of what are called fluxoids or vortices) until, at sufficiently high magnetic field strengths, the material reverts to being a nonsuperconducting solid.

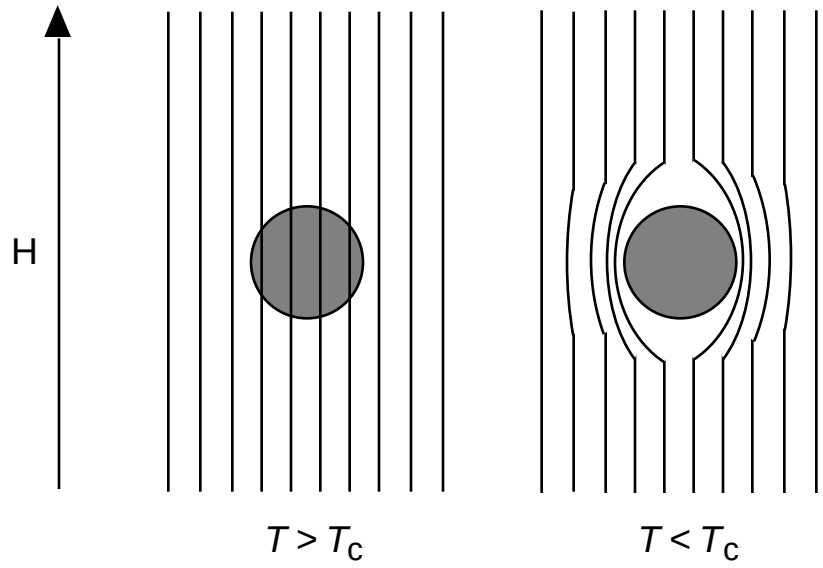

Figure 9.15. The Meissner effect. A superconductor (shaded circle) expels magnetic field lines from its interior.

In order to appreciate how the Meissner effect operates to produce levitation, some of the principles of electromagnetism will be reviewed. As recently as the beginning of the 19th century, electricity and magnetism were believed to be two separate phenomena. In 1820, however, the Danish physicist H. C. Oersted observed a connection between them. As illustrated in Figure 9.16, Oersted found that when he passed an electric current through a wire, a deflection was observed in the magnetic pointer of a compass; in other words, the current had induced a magnetic field. Electromagnets are based on this principle: A magnetic field is induced by passing current through a coil of wire. The very strong magnetic fields produced by passage of a large current through superconducting coils of wire will persist indefinitely in a closed circuit if the wires remain below T_c, because there is no resistance to the flow of current. This effect can be noted in superconducting magnets such as those in modern NMR spectrometers and magnetic resonance imaging (MRI) instruments. Once initiated, the current in a superconducting magnet will continue for years. However, loss of cooling will eventually produce "quenching" of the magnet; if a large current is flowing when superconductivity is lost, resistive heating will quickly boil off the coolant.

Following Oersted's observations, two other scientists, Michael Faraday and Joseph Henry, investigated the related question of whether a magnetic field could induce a current in an electrical conductor. They found that a magnet could induce a current if a magnet in a coil of wire was constantly in motion (or more fundamentally, if the magnetic flux linking the coil is continuously changing), as shown in Figure 9.17. Our present large-scale electrical energy needs are now met by generators that work on this principle.

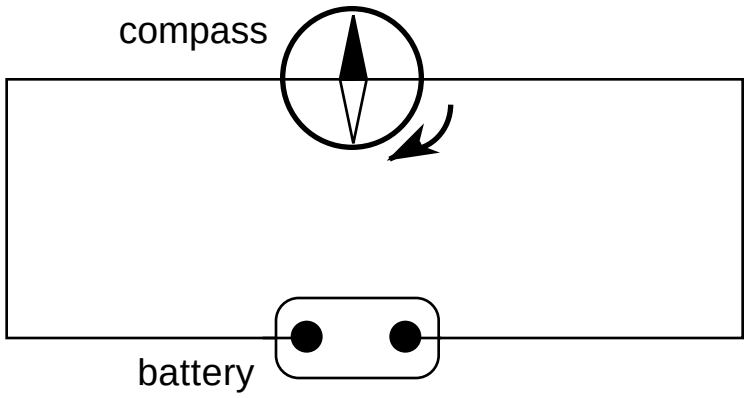

Figure 9.16. Oersted's experiment. The magnetic needle of a compass placed beneath a conductor carrying current will be deflected by the induced magnetic field.

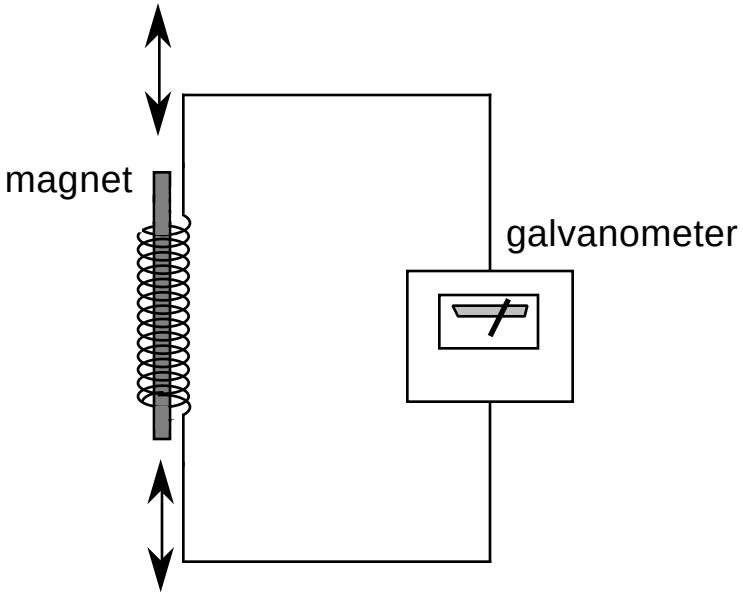

Figure 9.17. Moving a magnet through a coiled wire induces a current (more accurately, a voltage is induced, which drives the current), detected with a galvanometer.

The coupling of electrical and magnetic phenomena is elegantly demonstrated in a levitation experiment. As will be described, if a superconducting pellet is cooled below its critical temperature and a light, strong magnet is placed above the pellet, it hovers over the pellet (*see* Figure 9.18). The magnet retains this position so long as the pellet remains superconducting; once the pellet warms to its normal state, the magnet will no longer remain suspended in air.

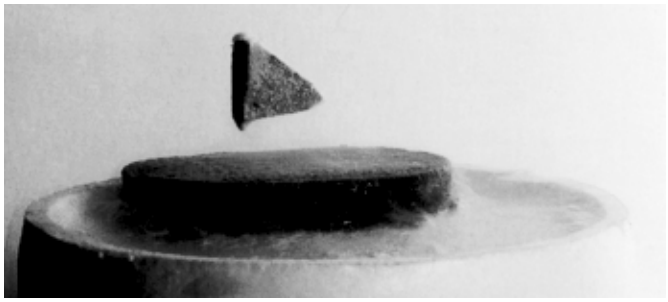

Figure 9.18. Levitation of a magnet above a liquid-nitrogen-cooled sample of $YBa_2Cu_3O_{7-x}$. The pellet is sitting atop an inverted Styrofoam cup.

Why does levitation occur? As the magnet approaches the pellet, it will induce a resistanceless supercurrent in the surface of the superconductor. For Type I superconductors, the supercurrent induces its own magnetic field that opposes the external magnetic field. This induced magnetic field leads to cancellation of the magnetic field inside the superconductor, accounting for the perfect diamagnetism of Type I superconductors. However, Type I superconductors do not provide stable levitation: The opposing magnetic fields from the superconductor and magnet can lift the magnet, but there is no force to prevent the lateral movement of the magnet.

In contrast, Type II superconductors provide a mechanism for stable levitation. The magnetic field lines that penetrate the sample resist motion, and thus keep the magnet in a fixed position. The height at which the magnet is levitated reflects the tendency to minimize the total energy of the system: the internal energy of the superconductor will increase as the magnet gets closer to the surface and more magnetic field lines enter the solid; and the gravitational potential energy will increase as the magnet gets further away from the surface. The levitation height reflects the minimum total energy based on the sum of these two contributions.

Demonstration 9.7. Levitation

Materials

Superconducting pellet (*see* Supplier Information)
Styrofoam cup
Strong, small magnet
Liquid nitrogen
Nonmagnetic tweezers

Procedure

- Cool a pellet of the 1-2-3 superconductor with liquid nitrogen using a Styrofoam stand (an inverted coffee cup, for example). **CAUTION: Liquid nitrogen is extremely cold. Do not allow it to come into contact with skin or clothing, as severe frostbite may result. Wear gloves when transferring and using liquid nitrogen.**
- Place a magnet on top of the superconducting pellet using the nonmagnetic tweezers. A standard refrigerator magnet, if small enough, can become airborne. However, the lift is more dramatic with strong, rare-earth-based magnetic compounds like $SmCo_5$ and $Fe_{14}Nd_2B$.
- Spin the levitated magnet. Marking one side with white correction fluid makes the spinning more visible.

Variations

- The experiment can be demonstrated before a large audience by placing an overhead projector on its back and taping, to the lens of the projector, the base of a plastic frame that holds a rotatable mirror. A schematic diagram of the mirror attachment and a picture illustrating its use appears as Appendix 9.2 to this chapter.
- If a small cylindrical magnet is available, a small fragment of another magnet can be attached to its corner. The cylindrical magnet can then be spun after levitation, and its rotation will be evident on the screen from the movement of the magnet fragment that is attached to it.
- The Meissner effect may also be demonstrated by using an enclosed balance in a manner similar to that shown in Figure 2.10. In this case, however, a sample of superconducting material in a cup containing liquid nitrogen is placed on top of the balance lid. The superconducting material repels a magnet supported on a stack of Styrofoam cups on the balance pan and induces a measurable weight change *(30)*.

The Mechanism of Superconductivity

Superconductivity baffled theorists for many years after its discovery. It was not until the late 1950s, some 40-odd years after Kamerlingh Onnes' experiments, that a satisfactory theory was found. Called the BCS theory after its authors, J. Bardeen, L. Cooper, and J. R. Schrieffer, it satisfactorily accounts for virtually all of the properties of the traditional, low-T_c superconductors (*31*). The cornerstone of the theory is a notion that at first seems counterintuitive: electrons are attracted to each other to form what are called Cooper pairs.

That two electrons, both negatively charged, would feel an attraction seems to violate electrostatic principles. The key to the attraction, though, is that it is mediated by the crystal. Positive ions, whose positions are fixed in the crystal, result in any metal because the valence electrons of atoms composing the metal have been removed from their individual atoms and move about freely (Chapter 7). Figure 9.19 shows that, as these electrons responsible for conductivity travel past the positive ions, the ions are drawn toward the path of the electron by electrostatic attraction. And because the ions are much more massive than the electrons and move more sluggishly, this “wake” of displaced positive charge persists long enough to attract a second electron, and thus forms the Cooper pair. The pair is thus bound by the mutual attraction of each electron for the positive ions in the crystal. Important characteristics of the Cooper-pair electrons are that their spins are paired and the combined momentum of the pairs is not affected by electron scattering. Consequently, scattering does not provide the energy transfer between the electrons and the atoms in the crystal that produces resistance in a normal conductor. In the superconducting state most of the conduction electrons are bound in Cooper pairs.

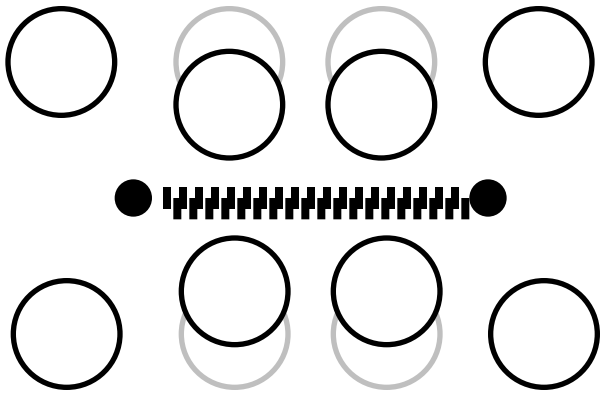

Figure 9.19. The coupling (dashed line) of two electrons (dark circles) into Cooper pairs is mediated by the crystal atoms (open circles), whose positions are affected by electronic motion. The atomic positions shift toward the electrons as they pass by; the original positions are indicated with the lighter outlines. Electrons in Cooper pairs exchange partners frequently.

A crude way to think of these pairs is as diatomic molecules. Like such molecules, they can be dissociated if sufficient energy is present to disrupt the bonding. The value of T_c is a reflection of this energy: as a superconductor is warmed, the number of Cooper pairs drops as T_c is approached.

Temperature is not the only experimental parameter that can affect the formation of Cooper pairs. As already noted, when magnetic fields are applied to a superconductor, supercurrents will be induced in the surface of the solid. If these fields and corresponding currents are sufficiently large, they can impart so much energy to the superconductor that the Cooper pairs will be dissociated and the superconductivity destroyed. Many potential applications of superconductors are precluded by the critical field H_c (and corresponding critical current J_c) at which this conversion from superconducting to normal behavior occurs.

Chemical Properties of a High-T_C Superconductor

Synthesis and Oxidation States

Making pellets of $YBa_2Cu_3O_{7-x}$ ($x \lesssim 0.1$) is straightforward, although several steps are involved *(32, 33)*. In a typical procedure, Y_2O_3, $BaCO_3$, and CuO are ground together and heated to about 950 °C. After cooling, pellets can be pressed and then sintered at 950 °C. Sintering involves heating just below the melting point; this process promotes bonding between the grains composing the pellet, thereby increasing the density and strength of the pellet (*see* Chapter 10). Once the pellet has been sintered, it is heated in oxygen at 500–600 °C and slowly cooled to room temperature.

The oxygen content of 1-2-3 has been estimated by standard chemical methods, which indicate it to be a compound having variable stoichiometry: Instead of having an integral number of oxygen atoms, the best superconducting materials appear to have values of x of about 0.1 or less. As has been discussed in Chapters 3 and 6, compounds with variable stoichiometry are common in the solid state and reflect chemistry associated with crystal defects.

Formal oxidation states can be assigned to the elements composing 1-2-3. Based upon the normal oxidation states of –2 for the oxide oxygen atom, +3 for the yttrium atom, and +2 for each barium atom, the resulting average oxidation state for each copper atom is 7/3 (for $x = 0$). The nonintegral oxidation state can be interpreted to mean that, on average, two-thirds of the Cu is present in Cu^{2+} sites in the crystal and one-third of the Cu is in Cu^{3+} sites.

Given the large number of elements that form oxides and the difficulty in predicting which of these combinations will form new phases, it is perhaps not surprising that 1-2-3 had not been prepared before. Since its discovery, however, thousands of related solids have been prepared. The

kind of chemical tuning discussed in connection with solid solutions and periodic properties (Chapters 3 and 7) has been attempted through substitutions for Y, Ba, and Cu. A variety of rare earth elements have been substituted for Y without greatly disturbing the superconducting characteristics of the material. However, substitution for Ba or Cu adversely affects superconductivity *(34)*.

Structure

X-ray diffraction studies (Chapter 4) have established that the 1-2-3 compound is structurally similar to the perovskite family, which is discussed in Chapter 5. Perovskites characteristically have a ratio of two metal atoms for each three oxygen atoms. Representative compounds with the perovskite structure are $CaTiO_3$, $NaNbO_3$, and $LaAlO_3$; in these simple perovskites the metal oxidation states must sum to +6 in order to yield an electrically neutral compound. Figure 5.28 gives the solid-state structure for the mineral perovskite, $CaTiO_3$, which has the larger Ca^{2+} cation in the center of the cubic unit cell, the smaller Ti^{4+} ions at each corner of the cube, and the O^{2-} ions bisecting the edges of the cube.

If 1-2-3 had an idealized perovskite structure, it would possess nine oxygen atoms in its formula (metal-to-oxygen atom ratio of 2:3) and would have the triple-decker structure sketched in Figure 5.29B. The resulting idealized unit cell, consisting of three stacked cubic unit cells, is now tetragonal rather than cubic, having a square base but rectangular sides. The top and bottom compartments of the tetragonal unit cell contain Ba^{2+} ions, and the middle compartment contains a Y^{3+} ion. The Cu ions occupy the corners of the cubes composing the unit cell, and the oxide ions again bisect the cube edges.

Why is the ideal structure not adopted by the 1-2-3 oxide? The answer may lie in the excessively high oxidation state required of Cu. A formula of $YBa_2Cu_3O_9$ leads to an average copper oxidation state of 11/3, which implies contributions from both Cu^{3+} and Cu^{4+} oxidation states. The fact that tetravalent Cu compounds are extremely rare strongly suggests that the average Cu oxidation state must be +3 or less. One avenue for achieving a lower oxidation state is to expel oxygen atoms from the crystal, giving the formula $YBa_2Cu_3O_7$ and a formal oxidation state of 7/3 for copper.

How the structure is tuned by varying the oxygen content is illustrated in Figure 5.29C. Although it is difficult (because of crystal disorder problems) to locate all of the oxygen atoms in the structure, the general geometrical pattern appears to be that 4 of the 12 oxide ions surrounding the Y^{3+} ion have been lost as well as four other oxide ions, two from the top face of the unit cell and two from the bottom.

These oxygen vacancies are defects in the crystal that are governed by chemical equilibria (Chapters 6 and 8). The solid can be regarded as a solvent wherein vacancies act as solutes that are subject to the same kinds of equilibrium expressions used to describe acid–base chemistry (Chapter 8). In this case, the concentration of oxygen vacancies is coupled

to the oxidation states of the copper ions composing the solid: As the oxygen content declines, so too does the average copper oxidation state. Specifically, because the solid must remain electrically neutral, each oxide ion that is removed requires compensatory removal of two units of positive charge; this compensatory removal can be accomplished if, for example, two Cu^{3+} centers are converted to Cu^{2+} centers. An equation describing the equilibrium that couples oxygen vacancies, V, with Cu oxidation states is,

$$2\ Cu^{3+} + O^{2-} \rightleftarrows 2\ Cu^{2+} + 1/2\ O_2\ (g) + V$$

The oxygen vacancies in 1-2-3 create sheets and chains of copper atoms (*see* Figure 5.30), linked through the remaining oxygen atoms, that may play a critical role in the superconductivity of the solid. One consequence of this bonding arrangement is that the physical properties of the material, including superconductivity, will show anisotropy, that is, they are dependent on the crystal direction along which they are measured.

Other Superconductors

Efforts to find new families of superconductors continue. After the discovery of 1-2-3, superconductors with critical temperatures as high as ~120 K were found with compositions of $Bi_2Ca_2Sr_2Cu_3O_{10}$ (T_c of 110 K) and $Tl_2Ca_2Ba_2Cu_3O_{10}$ (T_c of ~125 K). Table 9.1 lists a variety of ceramic superconductors and their critical temperatures.

Table 9.1. Examples of Oxide- and Fullerene-Derived Superconductors

Compound	T_c (K)	Reference
$YBa_2Cu_3O_{7-x}$	95	29
$Bi_2Sr_2CuO_6$	9	35
$Bi_2(Sr,Ca)_2CuO_6$[a]	80	36
$Bi_2Sr_{2.7}Ln_{0.3}Cu_2O_8$[b]	80	37
$Bi_2Ca_3Sr_2Cu_4O_{10}$	90	38
$Bi_2Ca_2Sr_2Cu_3O_{10}$	110	39
$Tl_2Ba_2Ca_2Cu_3O_{10}$	125	40
K_3C_{60}	18	41
K_2RbC_{60}	22	42
Rb_2KC_{60}	24	43
Rb_3C_{60}	29	43

[a] Sr and Ca form a solid solution.
[b] Ln = Y, Pr, Nd, Sm, Eu, Gd, Tb, Dy, Ho, Er, or Tm.

More recently, C_{60} was found to react with some of the alkali metals to form solids of composition M_3C_{60} (M = K, Rb, or Cs) that are superconducting with critical temperatures on the order of 30 K. In this structure, the C_{60} molecules form a fcc structure and the cations fill all of the tetrahedral and octahedral holes (*recall* from Chapter 5 that there are

two tetrahedral holes and one octahedral hole for each close-packed sphere, which in this case is a C_{60} molecule), and this behavior leads to the indicated stoichiometry. Some of these superconducting solids are also included in Table 9.1.

Applications

Applications of superconductors, at least in principle, increase with critical temperature. This situation results from the fact that liquid helium can be obtained at relatively few sites, whereas liquid nitrogen is readily available; the ease and efficiency of coolant transfer and storage are also greater for liquid nitrogen. Taken one step further, the discovery of a room-temperature superconductor has the potential to bring superconductive devices into every household. Whether these applications come to fruition will depend on whether some formidable problems in the realm of materials science can be overcome.

Focusing on 1-2-3 and related oxides, their brittle nature, characteristic of ceramics, represents a significant challenge if useful shapes like wires, ribbons, and films that are needed for electromagnetic applications are to be fabricated. For example, thin films have potential for use in SQUIDS (superconducting quantum interference devices, which are used for the measurement of very weak magnetic fields) and infrared sensors. Films with critical current densities as high as nearly 10^8 A/cm^2 have been prepared; such films can be grown on the surface of $LaAlO_3$ crystals using synthetic methods that include sputtering, molecular beam epitaxy, and chemical vapor deposition (Chapter 10), followed by treatments in controlled oxygen atmosphere. Films as thin as a few tens of angstroms have been prepared this way.

Superconducting wires and tapes have the mechanical and electrical properties necessary for use in electromagnets and superconducting motors. They are made by a process in which silver tubes are filled with fine powders of $Bi_2Sr_2Ca_2Cu_3O_{10}$ and minor amounts of other constituents that promote crystal growth at elevated temperatures. The filled tubes are drawn into wires, heat-treated, redrawn, and finally treated with oxygen (which diffuses through the silver to produce the correct oxygen stoichiometry in the superconductor). It is remarkable that superconductors that form crystals that are as brittle as glass have been incorporated into flexible wires as long as 100 m!

Commercially successful superconducting wires or tapes must be able to carry a current density of at least 10^4 A/cm^2, and, in some cases, they must retain this capacity when exposed to a strong magnetic field. For example, power transmission cables operate in a low magnetic field, but wires in generators or in magnets are exposed to fields of several teslas (1 tesla is 10,000 G; a refrigerator magnet's strength is on the order of 0.1 G). Some experimental samples of the new superconducting wires exhibit critical current densities of 50,000 A/cm^2 at 20 K compared to 10,000 A/cm^2 for Nb_3Sn wire, the wire used in present commercial applications. Given the substantial progress that has already been made in overcoming

fabrication problems, applications of the high-temperature superconductors may await in such diverse areas as the transmission of electrical power, electronics, and magnet-intensive technologies.

The ability of a superconductor to support a resistanceless direct current can be exploited in the lossless transmission of electrical power. At present, a significant fraction of generated electricity is lost as heat through the resistance associated with traditional conductors. Whether the conventional transmission of electricity will be affected by the superconducting ceramic is difficult to assess. Some loss of energy occurs when alternating current, the form of current provided by utilities, is being transferred. A large-scale shift to superconducting technology will also hinge on whether wires can be prepared from the ceramics that retain their superconductivity at 77 K, while supporting large current densities.

Other potential applications of the new superconductors appear in the field of electronics. For example, miniaturization and increased speed of computer chips are limited by the generation of heat and the charging time of capacitors arising from the resistance of the interconnecting metal films. The use of the new ceramics may result in more densely packed chips that could transmit information orders of magnitude more rapidly.

Superconducting electromagnets are an enabling component of several technologies. NMR spectroscopy, one of the most powerful tools for structural characterization in synthetic chemistry, and magnetic resonance imaging (MRI), which is playing an increasingly prominent role in medicine, both rely for their sensitivity on the intense magnetic fields provided by superconducting electromagnets. Levitated vehicles have been designed that employ superconducting magnets (Protoypes like the “mag-lev” train in Japan operate by inducing currents in metal train tracks (eddy currents) and not by the Meissner effect). Similarly, the particle accelerators that serve the high-energy physics community are dependent on high-field superconducting magnets. A controversy that surrounded the Superconducting Super Collider (SSC) also illustrates the political ramifications of new technologies. At issue was whether the multi-billion-dollar project should be constructed using the established liquid-helium-based superconducting technology, or whether construction should be postponed to embrace the developing liquid-nitrogen-based technology. Eventually the former view prevailed.

Ionically Conducting Copper Mercury Iodide

Unlike the 1-2-3 superconductor, which conducts electricity by electronic motion, the salt Cu_2HgI_4 (and the related solid, Ag_2HgI_4) is a good ionic conductor of electricity at temperatures a little above room temperature, where it undergoes an order–disorder phase change. The compound is easily prepared, and its phase change is observable both by increased conductivity and a color change. Other ionic conductors are described in Chapter 8.

Structure and Phase Change

The low-temperature ordered structure of Cu_2HgI_4 is shown in Figure 9.20C. Although the overall unit cell is tetragonal, with square bases and rectangular sides, it can be viewed as two fcc cells of iodide ions, with one cube atop the other. The iodide ions are in the fcc unit cells in the same positions as the sulfur atoms in ZnS (sphalerite form, *see* Chapter 5). All of the Cu^+ and Hg^{2+} cations are in tetrahedral holes of the structure that are formed by the iodide ions (there are two such holes for each iodide (Chapter 5), hence three-eighths of these holes will be occupied by the cations), but with a particular ordering (*see* Figure 9.20) *(42)*. In this low-temperature phase, the solid is brick red.

At a temperature of about 67 °C, disorder sets in, and the cations are randomly distributed about all of the tetrahedral holes in the structure. The phase change is accompanied by a color change to red–brown and a marked increase in electrical conductivity. The color change is due to a small decrease in the band gap (2.1 to 1.9 eV) with the change in structure *(43)*. In this high-temperature phase, the unit cell is a cube, because the X-ray diffraction experiment (Chapter 4) measures the average occupation of the tetrahedral sites, and the disorder makes it appear that, on average, each tetrahedral site contains one-fourth of a copper ion and one-eighth of a mercury ion.

Conductivity Mechanism

Above the transition temperature, Cu_2HgI_4 exhibits ionic conductivity (with some electronic conductivity also). Five-eighths of the tetrahedral holes and all of the octahedral holes formed by the iodide ions are vacant, and these open sites provide possible pathways for the small copper cations to move through the crystal, carrying charge. It is easiest for a copper cation to jump between tetrahedral holes by moving to an octahedral hole and then to the new tetrahedral hole, rather than jumping directly between tetrahedral holes.

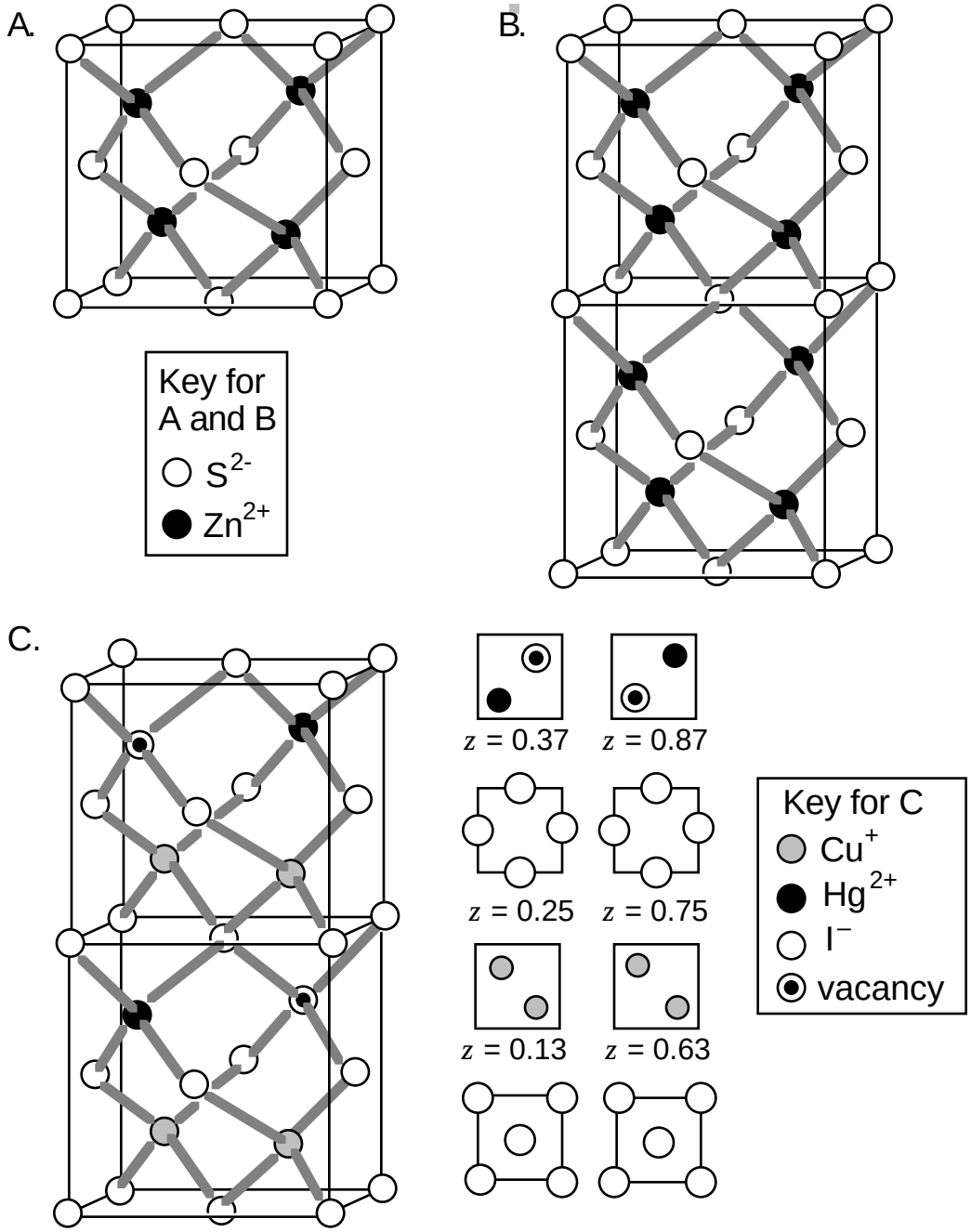

Figure 9.20A–C. The structure of Cu_2HgI_4 is related to the structures of ZnS (sphalerite) and of CaF_2 (fluorite). A: A sphalerite unit cell. B: Two stacked sphalerite unit cells. C: The ordered (low-temperature) structure of Cu_2HgI_4, with the *z* layer sequence. Three-eighths of the tetrahedral holes are occupied (2 of the 10 vacancies are shown; *see* the fluorite-like structure in D).

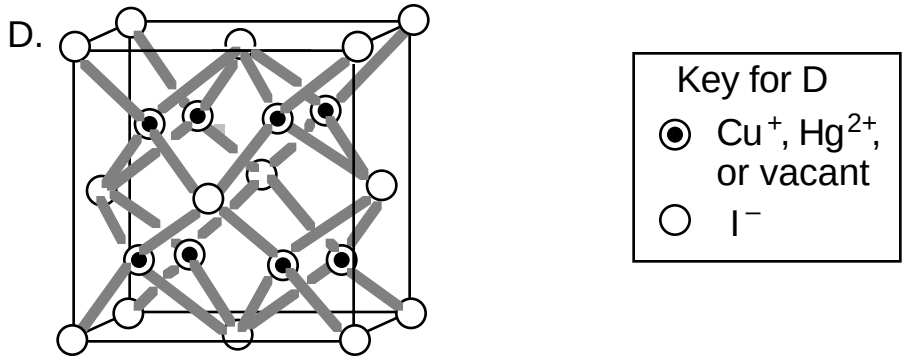

Figure 9.20D. The disordered (high-temperature) structure of Cu_2HgI_4. The cations are randomly distributed throughout all of the tetrahedral holes.

Demonstration 9.8. The Order–Disorder Phase Change in Copper(I) Mercury(II) Iodide

Materials

Cu_2HgI_4 (Samples are readily prepared from CuI, $Hg(NO_3)_2$, and KI; *see* Experiment 12 for the procedure)
Two glass plates or watch glasses (the watch glasses should be of the same size and curvature)
Spatula
Filter paper
Glue or tape
Heat gun
Insulated gloves

Procedure

- Using a spatula, rub some of the red Cu_2HgI_4 powder into a piece of filter paper. Sandwich the paper between two glass plates or watch glasses and glue or tape them together.
- Pick up the glass-encased sample while wearing thermal gloves and blow hot air from a heat gun onto the glass. The color change to red–brown will be readily apparent and, as the sample cools, its red color will return.

Caution: Mercury compounds are toxic. Avoid skin contact and inhaling dust from the compound. Place the waste from this demonstration in an appropriately labeled container and dispose of it according to state and local regulations.

Demonstration 9.9. Conductivity Changes in Cu_2HgI_4

Materials

Cu_2HgI_4
4-cm length of 4-mm o.d. glass tubing
Two brass L-shaped electrodes of about 2.5-mm diameter with wires attached
Rubber band
Ohmmeter and leads
Heat gun or matches

Procedure

- Assemble the apparatus for demonstrating the temperature-dependent conductivity of Cu_2HgI_4, as shown in Figure 9.21.
- Insert one electrode almost half way into the glass tube. Introduce a small portion of Cu_2HgI_4 into the other end, ensuring that there is enough sample in the glass tube so that the ends of the brass Ls will not touch (touching would short the circuit). When packed, the distance between the electrodes should be between 2 and 5 mm.
- Insert the second electrode. Hold the electrodes in place by stretching a rubber band around them.
- Connect the assembled conductivity apparatus in series with an ohmmeter, as shown in Figure 9.21. A heat gun or a match can be used to heat the Cu_2HgI_4.
- As the sample is heated, monitor the resistance. It will decrease, a result indicating that the conductivity is increasing. Upon cooling, the resistance will return to its original value, an effect reflecting the reduced conductivity of Cu_2HgI_4 at room temperature. **Caution: Mercury compounds are toxic. Avoid skin contact and inhaling dust from the compound. Place the waste from this demonstration in an appropriately labeled container and dispose of it according to state and local regulations.**

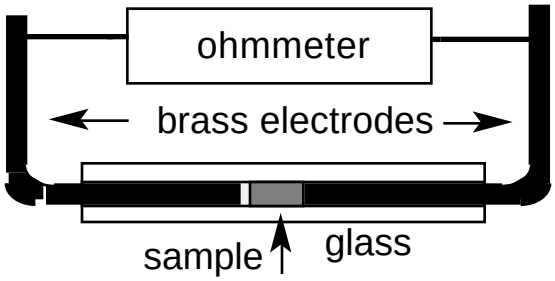

Figure 9.21. An apparatus to measure the conductivity in Cu_2HgI_4.

Laboratory. The synthesis and properties of Cu_2HgI_4 are presented in Experiment 12.

Appendix 9.1. Prediction of Shifts in Equilibria

As noted in the chapter, the phase of a pure material with the lowest free energy (G) at a given pressure (P) and temperature (T) will be the most stable phase. From thermodynamics,

$$dG = V\,dP - S\,dT$$

where V is molar volume and S is entropy. The predictions of Le Chatelier's principle are based on temperature- and pressure-induced changes in the free energies of a pure material.
The slope of a plot of molar free energy versus temperature at a given pressure is the negative of the molar entropy of the phase.

$$\text{at constant } P, \text{ slope } \frac{dG}{dT} = -S$$

Figure 9.22A illustrates a typical free energy versus temperature plot. Although the solid is more stable at low temperature, the difference in slopes means that as the temperature increases, the liquid phase approaches the solid phase in stability. At the melting (crossover) point the two phases have equal free energies, and above this temperature the liquid phase has the lower free energy and is more stable. (The slight curvature of the lines occurs because the entropy is not constant but increases with temperature).

The free energy of a pure phase increases with an increase in pressure, and the slope of a plot of molar free energy versus pressure at a given temperature is the molar volume of the phase.

$$\text{at constant } T, \text{ slope } \frac{dG}{dP} = +V$$

Figure 9.22B shows a typical plot of free energy versus pressure. Although the liquid is more stable at low pressure, the difference in slopes means that as the pressure increases, the solid phase approaches the liquid phase in stability. At the melting (crossover) point the two phases have equal free energies, and above this pressure the solid phase has the lower free energy and is more stable. (The slight curvature of the lines occurs because the molar volume is not constant but decreases with increasing pressure).

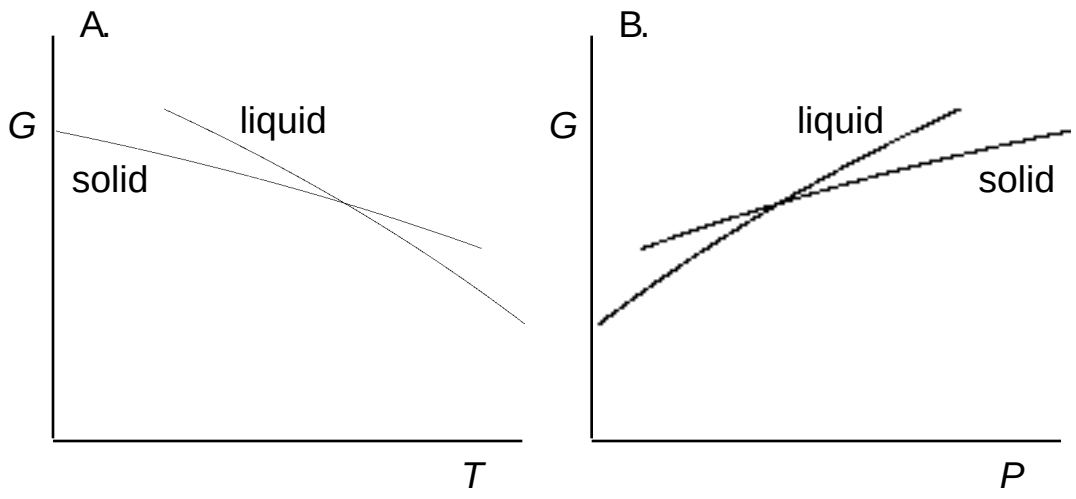

Figure 9.22. Plots of free energy versus temperature (A) and free energy versus pressure (B) for a typical material.

Ice and water are familiar materials that behave differently. The plots of G versus T and G versus P for H_2O are shown in Figure 9.23. In the plot of free energy versus temperature (Figure 9.23A), liquid water has the steeper slope, reflecting its higher entropy. The free energy versus pressure plot for liquid water and ice (Figure 9.23B) shows the anomalous behavior of this substance. Because ice has the greater molar volume, its curve has the steeper slope, meaning that with increasing pressure the denser, liquid phase becomes more stable. This situation is the reverse of the more typical situation shown in Figure 9.22B.

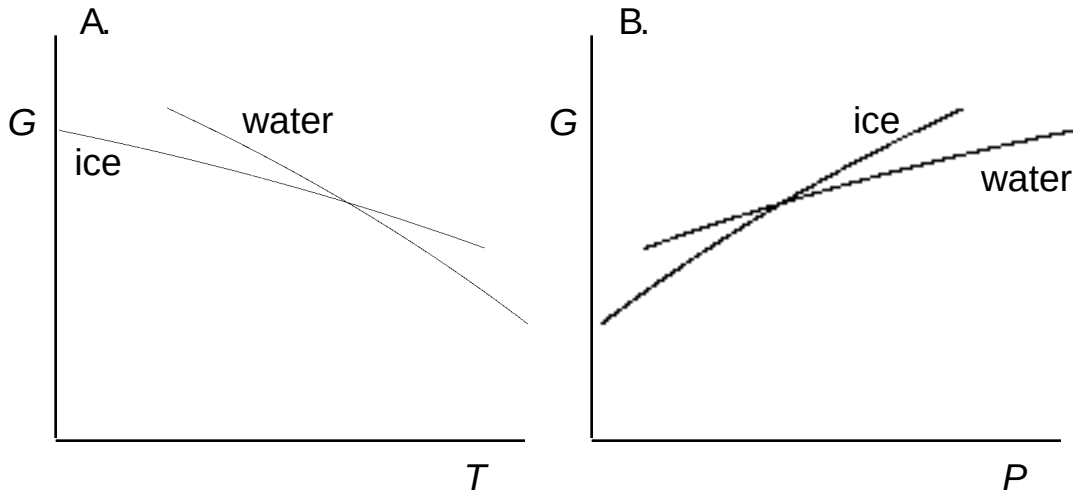

Figure 9.23. Plots of free energy versus temperature (A) and free energy versus pressure (B) for H_2O.

An alternative way to illustrate the effects of temperature and pressure on free energy is to superimpose the pressure effect on Figure 9.22A. This approach is illustrated for the general case in Figure 9.24A. The thicker lines in this figure correspond to the increased free energy for each phase caused by an increase in pressure. The increase is larger for the phase with the larger molar volume (the liquid), and shows that pressure applied to the solid can increase its melting point: the crossover point for the solid and liquid curves moves to higher temperature. Figure 9.24B shows this same plot for H_2O. In this case, the increase in free energy is larger for the solid (ice) and shows that the crossover point moves to lower temperature for this substance, corresponding to a lower melting point with increased pressure.

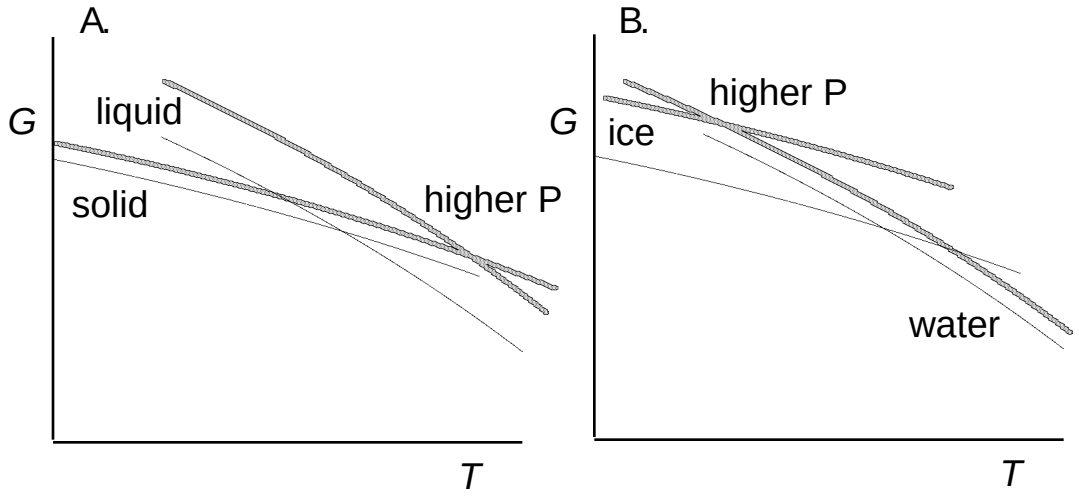

Figure 9.24. Free energy versus temperature at two different pressures for a typical material (A) and for H_2O (B). The thicker curves correspond to higher pressure for each phase.

Appendix 9.2. Construction of the Projector Mirror

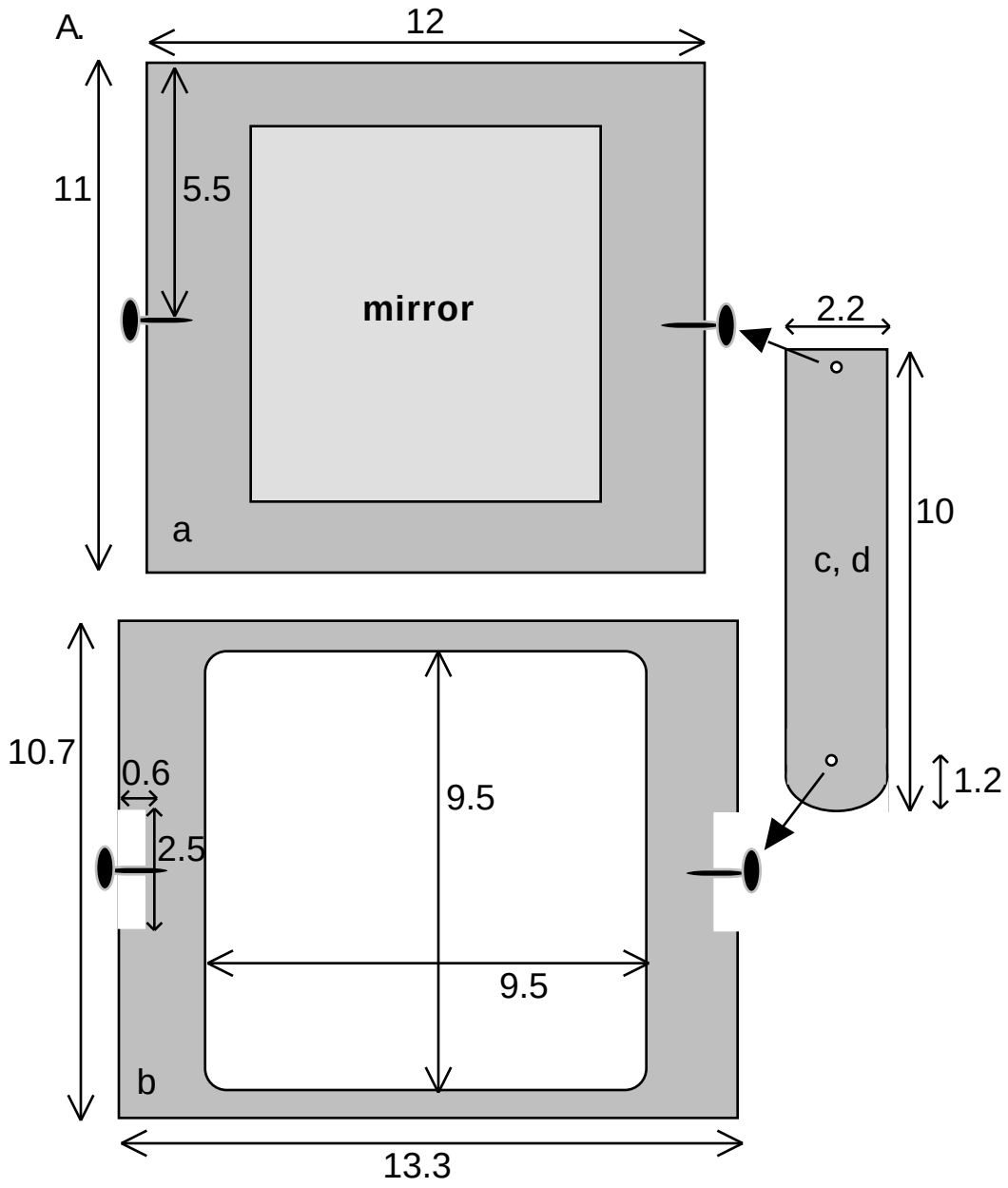

Figure 9.25A. A schematic diagram for a mirror attachment that can be used to display the superconductor levitation experiment with the overhead projector. Pieces a and b are made out of 9-mm thick Plexiglas, and pieces c and d are made out of 5-mm thick Plexiglas. All dimensions given in the diagram are in centimeters. The mirror shown in A is inlaid into the Plexiglas. Four plastic-knobbed thumbscrews are used to connect the pieces. Tapped holes are required for the screws.

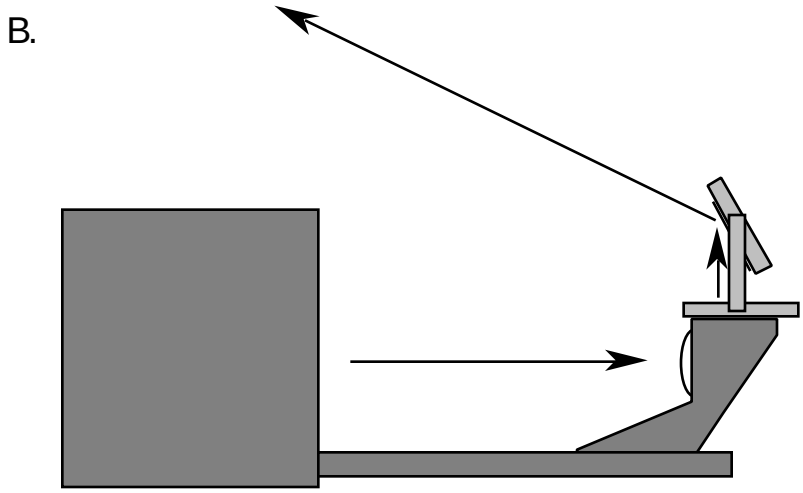

Figure 9.25B. A schematic diagram showing how the mirror attachment and an overhead projector are placed so as to demonstrate levitation. The overhead projector is placed on its back, and the mirror attachment is taped to the head of the projector. The angle of the mirror is adjusted until the image is on the screen. The superconductor is placed on a stand or set of books so that it sits in roughly the middle of the projector glass.

References

1. Shakhashiri, B. Z. *Chemical Demonstrations: A Sourcebook for Teachers*; University of Wisconsin Press: Madison, WI, Vol. 3, 1989, p 310.
2. Louks, L. F. *J. Chem. Educ.* **1986**, *63*, 115–116.
3. Silberman, R. *J. Chem. Educ.* **1988**, *65*, 186.
4. *Mellor's Modern Inorganic Chemistry*; Parkes, G. D., Ed.; Wiley: New York, 1967, p 786.
5. Machlin, E. S. *An Introduction to Aspects of Thermodynamics and Kinetics Relevant to Materials Science*; Giro Press: Croton-on-Hudson, NY, 1991, p 25.
6. Shakashiri, B. Z. *Chemical Demonstrations: A Sourcebook for Teachers*; University of Wisconsin Press: Madison, WI, 1983, Vol. 1, pp 27–33.
7. Based on an in-press paper in *J. Chem. Educ.* by Gisser, K. R. C.; Geselbracht, M. J.; Cappellari, A.; Hunsberger, L.; Ellis, A. B.; Perepezko, J.; Lisensky, G. C.
8. Collen, K. R.; Ellis, A. B.; Perepezko, J. H.; Moberly, W.; Busch, J. D. *Chemistry of Advanced Materials*; Rao, C. D. N., Ed.; Blackwell: London, 1992; p 197.
9. Wayman, C. M. *MRS Bull.* **1993**, *18 (4)*, 49–56.
10. Wang, F. E.; Buehler, W. T.; Pickart, S. J. *J. Appl. Phys.* **1965**, *36*, 3232.
11. Michal, G. M.; Sinclair, R. *Acta Cryst. B* **1981**, *37*, 18.
12. Kudoh, Y; et al. *Acta Metall.* **1985**, *33*, 2049.
13. Shimizu, K.; and Tadaki, T. In *Shape-Memory Alloys*; Funakubo, H., Ed.; Gordon and Breach: New York, 1984; p 7.

14. Geselbracht, M. J.; Penn, R. L.; Lisensky, G. C.; Stone, D. S.; and Ellis, A. B. "Mechanical Properties of Metals," *J. Chem. Educ.*, in press.
15. Murray, J. L. In *Phase Diagrams of Binary Titanium Alloys*; Murray, J. L., Ed.; ASM International: Metal Park, OH, 1987; p 203.
16. Bhatia, A. B. *Ultrasonic Absorption*; Oxford University Press: Oxford, England, 1987.
17. Chalmers, B. et al. In *Progress in Materials Science*; Warlimont, H.; Delaey, L., Eds.; Pergamon: Oxford, England; 1974; Vol. 18; p 104.
18. Collen, K. R.; Ellis, A. B.; Perepezko, J. H.; Moberly, W.; Busch, J. D. In *Chemistry of Advanced Materials*; Rao, C. D. N., Ed.; Blackwell: London, 1992; p 197.
19. Lindquist, P. G.; Wayman, C. M. In *Engineering Aspects of Shape Memory Alloys*; Duerig, T. W., Ed.; Butterworth: London, 1990; p 58.
20. Yi, H. C.; Moore, J. J. *J. Metals* **1990**, Aug., 31.
21. Honma, T. In *Shape-Memory Alloys*; Funakubo, H., Ed.; Gordon and Breach: New York, 1984; p 81.
22. Liu, X.; Stice, J. *J Appl. Manuf. Syst.* **1990**, Jan., 65.
23. Stoeckel, D.; Tinschert, F. *SAE Technical Paper Series 910805*; Society of Automotive Engineers: Warrendale, PA, 1991; p 145.
24. Deschamps, O. *J. Metals* **1991**, *43*, 64.
25. Ellis, A. B. *J. Chem. Educ.* **1987**, *64*, 836–841.
26. Ashcroft, N. W.; Mermin, N. D. *Solid State Physics*; Saunders: Philadelphia, PA, 1976; Chapter 34.
27. Bednorz, J. G.; Müller, K. A. *Z. Phys. B.* 1**986**, *64*, 189.
28. Wu, M. K., Jr.; Ashburn, J. R.; Torng, C. J.; Hor, P. H.; Meng, R. L.; Gao, L.; Huang, Z. J.; Wang, Y. Q.; Chu, C. W. *Phys. Rev. Lett.* 1**987**, *58*, 908.
29. Cava, R. J.; Batlogg, B.; van Dover, R. B.; Murphy, D. W.; Sunshine, S.; Siegrist, T.; Remeika, J. P.; Rietman, E. A.; Espinosa, G. P. *Phys. Rev. Lett.* **1987**, *47*, 1676.
30. McHale, J.; Schaeffer, R.; Salomon, R. E. *J. Chem. Educ.* **1992**, *69*, 1031–1032.
31. Rose-Innes, A. C.; Rhoderick, E. H. *Introduction to Superconductivity*, 2nd ed.; Pergamon: Oxford, England, 1978.
32. Juergens, F. H.; Ellis, A. B.; Dieckmann, G. H.; Perkins, T. R. I. *J. Chem. Educ.* **1987**, *64*, 851.
33. Grant, P. M. *New Sci.* **1987,** July 30, 36.
34. Dagani, R. *Chem. Eng. News* **1987**, *65* (May 11), 7.
35. Torardi, C. C.; Subramanian, M. A.; Calabrese, J. C.; Gopalakrishnan, J.; McCarron, E. M.; Morrissey, K. J.; Askew, T. R.; Flippen, R. B.; Chowdhry, U.; Sleight, A. W. *Phys. Rev. B* **1988**, *38*, 225.
36. Rao, C. N. R.; Ganapathi, L.; Vijayaraghavan, R.; Ranag Rao, G.; Murthy, K.; Mohan Ram, R. A. *Physica C* **1988**, *156*, 827.
37. Den ,T.; Akinitsu, J. *Jpn. J. Appl. Phys.* **1989**, *28*, L193.
38. Sleight, A. W.; Subramananian, M. A.; Torardi, C. C. *Mat. Res. Soc. Bull.* **1989**, *14* (1), 45.
39. Tarascon, J. M.; McKinnon, W. R.; Barboux, P.; Hwang, D. M.; Bagley, B.B.; Greene, L. H.; Hull, G. W.; Le Page, Y. *Phys. Rev. B* **1988**, *38*, 8885.
40. Torardi, C. C.; Subramanian, M. A.; Calabrese, J. C.; Gopalakrishnan, J.; Morrissey, K. J., Askew, T. R.; Flippen, R. B.; Chowdhry, U.; Sleight, A. W. *Science*, **1988**, *240*, 631.
41. Haddon, R. C. *Acc. Chem. Res.*, **1992**, *25*, 127–130, and references therein.
42. Hahn, H.; Frank, G.; Klingler, W. *Z. Anorg. Allg. Chem.* **1955**, *279*, 279–280.
43. Jaw, H-R. C.; Mooney, M. A.; Novinson, T.; Kaska, W. C.; Zink, J. I. *Inorg. Chem.* **1987**, *26*, 1387–1391.

Additional Reading

- *Chemistry of Superconductor Materials;* Vanderah, T. A., Ed.; Noyes Publications: Park Ridge, NJ, 1992.
- West, A. R. *Solid State Chemistry and Its Applications*; Wiley: New York, 1984, Chapter 13 (ionic conductors).

Memory Metal

- Kauffman, G. B.; Mayo, I. *Invention and Technology*. **1993**, *9* (Fall), 18–23.
- Wayman, C. M. *MRS Bull.* **1993**, *XVIII*, 49–56.

Acknowledgments

This chapter was written with the helpful assistance of Norman Craig, Oberlin College, Department of Chemistry; Frank Weinhold, University of Wisconsin—Madison, Department of Chemistry; and Don Murphy, AT&T Bell Laboratories.

We thank Olivier Deschamps; Atelier D'Art Public; 36 rue Serpente; 75006 Paris, France, for permission to use the photographs in Figure 9.12.

Exercises

1. Choose the correct answer. In the high-temperature phase of NiTi (the unit cell is shown in Figure 9.2), the coordination numbers of the Ni and Ti are
   a. 6 for Ni and 6 for Ti
   b. 6 for Ni and 8 for Ti
   c. 8 for Ni and 6 for Ti
   d. 8 for Ni and 8 for Ti

2. Choose the correct answer. In the phase change during which a material becomes a superconductor
   a. the solid becomes a liquid
   b. the material becomes more electrically resistive
   c. a magnetic field becomes concentrated inside the solid
   d. electrons in the solid pair up

3. What technique lets us determine the atomic positions in NiTi memory metal both before and after the solid has undergone its phase change?
   a. spectroscopy with visible light
   b. measurement of specific heat
   c. electrical resistivity
   d. X-ray diffraction

4. Suppose that you wish to make 12 g of the 1-2-3 superconductor.
   a. Write a balanced equation for the reaction.
   b. How many grams of each starting material (Y_2O_3, $BaCO_3$, CuO, O_2) are needed?

5. Design a device based on a compound such as Cu_2HgI_4 that is insulating at low temperatures but conducting above some threshold temperature.

6. Design a device based on a compound such as Cu_2HgI_4 that is one color at low temperatures but changes to a different color above some threshold temperature. (Such behavior is called thermochromism.)

7. Confirm the formula of Cu_2HgI_4 by examining the unit cell shown in Figure 9.20.

8. Shown in the table are thermodynamic data for white and gray tin; recall that these two forms of tin have very different structures and densities. Consider the reaction, white tin $\rightleftarrows$ gray tin.
   a. For 1 mol of tin, what is the free energy change for the reaction at 298 K, ΔG^o, and therefore in which direction does this reaction go spontaneously at 298 K?

Allotrope	ΔH_f^o (kJ/mol)	ΔG_f^o (kJ/mol)	S^o J/K-mol
White tin	0	0	51.55
Gray tin	–2.09	0.13	44.14

   b. It is often the case that the standard enthalpy and entropy of a reaction, ΔH^o and ΔS^o, respectively, are roughly constant over a broad temperature range. Making this assumption, at what temperature would you predict that the two forms of tin will be in equilibrium with one another (at what temperature will ΔG for the reaction equal zero)?

9. Why do purely solid-state phase changes like that exhibited by NiTi memory metal often involve enthalpies of only a few kilojoules of energy per mole compared to values like 40 kJ to vaporize a mole of water?

10. If a metal can exist in both the hcp and ccp structures, can pressure be used to convert one to the other? Why or why not? [This type of question can be asked of conversions involving any combination of sc, bcc, hcp, and ccp (= fcc) structures for metals; see the packing efficiencies in Table 5.1 to predict the results of an increase in pressure at a given temperature.]

11. Pellets of superconducting 1-2-3 can be used to levitate a magnet. Under what conditions can a magnet be used to levitate pellets of 1-2-3?

12. Figure 2.10 shows a change in measured weight resulting from the magnetic interaction of a paramagnetic or ferromagnetic solid with a magnet. How could a similar experiment be conducted with a pellet of superconducting 1-2-3 and what effect, if any, would this have on the measured weight?

13. How might a “double-decker” levitation experiment be conducted with superconductors and magnets, wherein one object is levitated above a second object, which is simultaneously levitated above a third object? Is a “triple-decker” levitation experiment feasible?

14. Silver mercury iodide, Ag_2HgI_4, undergoes a similar phase transition and corresponding enhancement in ionic conductivity as Cu_2HgI_4, albeit at a slightly lower temperature of about 47 °C. The high-temperature phases of the two solids have the same disordered zinc-blende-like structure. The low

temperature phase of the silver compound, shown as follows, differs from that of the copper compound only in the relative positions of the monovalent cations and vacancies. Show that the unit cell for the Ag_2HgI_4 solid corresponds to this stoichiometry. How do the positions of monovalent cations and vacancies differ in the two structures?

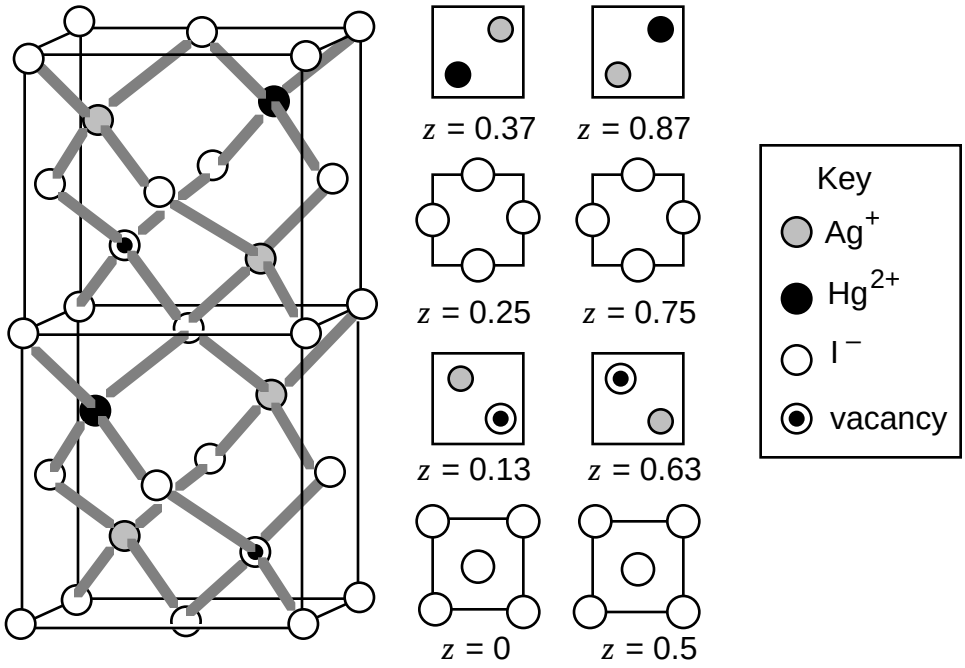

15. The colors of the two phases of Cu2HgI4 reflect their band structures. In both cases, the color is believed to arise from the network of tetrahedral HgI_4^{2-} units composing the solid. The lower energy filled band is derived primarily from filled iodide p orbitals: Which p orbitals are these? (What is the principal quantum number for these p orbitals?) The higher energy unfilled band is derived primarily from mercury s orbitals: Which orbitals are these?

16. Ag_2HgI_4 changes from yellow below the phase transition to orange above it. Interpret this change using Figure 7.18. The shift in the band gap has been interpreted as being due primarily to changes in the widths of the bands. If this is the case, how is the band width changing as the solid goes from the low- to the high-temperature phase? Similarly, Cu_2HgI_4 changes from red at room temperature to dark red–brown above the transition temperature. Interpret these changes in the manner used to describe the silver compound's phase change.

17. Analyze whether solid solutions of Ag_2HgI_4 and Cu_2HgI_4 can be expected to form in the high-temperature form. (Ionic radii are 0.74 Å for Cu^+ and 1.14 Å for Ag^+ in tetrahedral environments.) If so, how would you write the formula for the solid?

18. Determine the formal oxidation state for copper in the other superconductors of Table 9.2, assuming that the oxidation state for lanthanide elements, thallium and bismuth is +3; for oxygen, –2; and for alkaline earth elements, +2.

19. Design a sculpture made of memory metal that will change its shape using electricity. Why can this be done?

20. Using Figure 9.10, what compositions of Ni_xTi_{1-x} would you choose so as to have two samples, one of which is in the low-temperature phase at 0 °C, and the other of which is in the high temperature phase at this same temperature. How could you tell them apart without chemical analysis?

21. Samples of nickel–titanium can also be trained to have "two-way memory," wherein they reversibly adopt one shape in their low-temperature phase and a second shape in their high-temperature phase. This step is accomplished by holding the sample in the desired shape (holding a wire that is linear in its high temperature form in a V-shape, for example) at low temperature, and maintaining this shape at the higher temperature where the sample would normally go back to its high-temperature shape (to a straight line, in this case). If the sample is cycled through this process repeatedly, the two-way memory develops: in this example, the sample will be V-shaped when cool and linear when warm. What happens to the variants of the low-temperature phase during this processing treatment that permits the two-way memory? (See reference 9.)

22. When a thin straight wire of NiTi memory metal in the low-temperature phase is bent and placed in a concentrated solution of bromine in wet methanol, it straightens out as it dissolves. Why? Speculate on the reaction products.

23. Because NiTi memory metal is biocompatible, it has been proposed that it could be inserted into arteries to help unclog them. Given that the metal is to be coiled like a spring in one phase and straight in the other, how is the experiment carried out?

24. Potassium chloride can be converted from its normal rock salt structure to the cesium chloride structure under high pressure at 298 K. The reaction can be written KCl (rock salt structure) $\rightleftarrows$ KCl (cesium chloride structure). Which structure has the greater density? The greater molar volume?